UPPSALA
UNIVERSITET

Magnetic reconnection at the Earth's magnetopause: CLUSTER spacecraft observations at different scales

Licentiate Thesis
by

Alessandro Retinò
Department of Astronomy and Space Physics
Uppsala University
SE-75120 Uppsala, Sweden

October 12, 2005

Abstract

Magnetic reconnection is an universal process that changes the topology of the magnetic field and converts electromagnetic energy into energy of charged particles. The best laboratory to study in-situ magnetic reconnection is the Earth's magnetosphere. At the magnetopause, the boundary that separates magnetic field and plasma of solar wind origin from the terrestrial ones, magnetic reconnection enables the interconnection between the interplanetary magnetic field and the Earth's magnetic field thus allowing the transport of mass, momentum and energy from the solar wind into the magnetosphere. Reconnection is fast initiated in a microscopic region, the so-called diffusion region, where plasma and magnetic field are decoupled but affects very large volumes in space for a long time. Therefore it is a key point to study magnetic reconnection at different spatial and temporal scales.

The European Space Agency cornerstone Cluster mission is the first multispacecraft magnetospheric mission that allows an in-situ study of magnetic reconnection at various scales thanks to three-dimensional measurements at different spacecraft separation.

In this thesis we present Cluster spacecraft observations of magnetic reconnection at the dayside magnetopause. At large temporal (several hours) and spatial (several Earth's radii) scales we show that magnetic reconnection is continuous in time and that it best agrees with the component merging model. At scales smaller than an ion gyroradius we concentrate on observations close to the X-line and we study the microphysics of reconnection. We show that a separatrix region that is several ion inertial lengths λ_i wide can be identified between the magnetic separatrix, i.e. the magnetic field lines connected to the X-line, and the reconnection jet on the magnetospheric side of the magnetopause. The separatrix region is highly structured down to Debye length λ_D scales, even though the X-line can be up to several tenths of λ_i away.

Alessandro Retinò
Swedish Institute of Space Physics
Box 537
SE-751 21 Uppsala
Sweden
alessandro.retino@irfu.se

List of Papers

Papers included in the thesis:

Paper I

A. Retinò, M. B. Bavassano-Cattaneo, M. F. Marcucci, A. Vaivads, M. André, Y. Khotyaintsev, T. Phan, G. Pallocchia, H. Rème, E. Moebius, B. Klecker, C. W. Carlson, M. McCarthy, A. Korth, R. Lundin, *Cluster multispacecraft observations at the high latitude duskside magnetopause: implications for continuous and component magnetic reconnection*, Ann. Geophys., **23**, 461-473, 2005.

Paper II

A. Retinò, A. Vaivads, M. André, F. Sahraoui, Y. Khotyaintsev, M. B. Bavassano-Cattaneo, M. F. Marcucci, M. Morooka, J.S. Pickett, C.J. Owen, S.C. Buchert, N. Cornilleau-Wehrlin, *The structure of the separatrix region close to a magnetic reconnection X-line: Cluster observations*, Geophys. Res. Lett., submitted, 2005.

Papers not included in this thesis:

Paper III

A. Vaivads, Y. Khotyaintsev, M. André, **A. Retinò** , S.C. Buchert, B.N. Rogers, P. Décréau, G. Paschmann, T.D. Phan, *Structure of the magnetic reconnection diffusion region from four-spacecraft observations*, Phys. Rev. Lett., **93(10)**, 2004.

Paper IV

Y. Zheng, G. Le, J. A. Slavin, M. L. Goldstein, C. Cattell, A. Balogh , E. A. Lucek , H. Rme , J. P. Eastwood , M. Wilber, G. Parks, **A. Retinò** , A. Fazakerley, *Cluster observation of continuous reconnection at dayside magnetopause around cusp*, Ann. Geophys., accepted, 2005.

Contents

Introduction

A wind of charged particles, the so-called solar wind, continuously blows from our Sun towards the Earth's carrying along the solar magnetic field. If this wind could have had access to our atmosphere it could have blown it away much, as probably it happened with our neighbor planet Mars. Luckily for us, the Earth's magnetic field is providing a quite efficient shield against the solar wind. This shield is called the magnetopause. Under normal condition the magnetopause is impenetrable and we are safe. Nevertheless a small fraction of these particles can sometimes cross the magnetopause and come close to us. This is what happens for example when we see northern lights: charged particles of solar wind origin hit neutral particles in our atmosphere and produce beautiful light shows. This penetration is mainly possible because of something called *magnetic reconnection* that occurs at the magnetopause. There the solar magnetic field carried along by the solar wind interconnect with the Earth's magnetic field thus creating highways along which the solar particle can reach the Earth.

Though in a more complicated way, that's what we believe is happening at the Earth's magnetopause. In our research we try to understand how this process works in detail and try to answer some fundamental questions. How does magnetic reconnection create 'holes' at the magnetopause that instead should be impenetrable? How big are these holes and where are they located on the magnetopause? How long do they stay open? What's happening around them?

In the next chapters we will briefly show what magnetic reconnection is and how it works at the Earth's magnetopause. This has the goal to provide a basic framework for later reading the articles included in the thesis.

Chapter 1

The interaction between the solar wind and the Earth

A plasma is a gas of ionized particles that, on the average, is neutral. In a non-collisional plasma, the collisions between ions and electrons can be neglected, that means the mean free path is very large. In absence of collisions charged particles can move freely along the magnetic field as beads along nylon strings, but not much transversely to it. One often explains this saying that the magnetic field is 'frozen' in the plasma. This means that charged particles stay almost always attached to a given magnetic field line and cannot jump to the neighbor line, implying that when two different plasmas and magnetic fields come in contact they cannot mix.

The *solar wind* is a plasma stream continuously emitted from the Sun into the solar system. For the solar wind plasma the mean free path is ~ 1 AU ~ 150 millions of kilometers, thus it is a highly non-collisional plasma. This implies that the solar magnetic field is frozen into the solar wind plasma and is carried away from the Sun by the solar wind. Far away from the Sun one usually calls that field the *interplanetary magnetic field* (IMF).

The Earth, as other objects in the solar system, is an obstacle to the solar wind. Due to the supersonic velocity of the solar wind, a standing shock wave, the *bow shock*, is formed in front of the Earth. Downstream of the bow shock, in the *magnetosheath*, the shocked solar wind plasma is decelerated to subsonic velocity and it flows around the Earth.

Because of the Earth's magnetic field, the solar wind-Earth interaction is actually more complicated. Due to the frozen-in condition, the interplanetary and terrestrial magnetic fields cannot mix and a discontinuity surface, *the magnetopause*, develops between the two fields. In the anti-sunward direction the Earth's magnetic field is confined in a comet-like cavity, the *magnetosphere*. Figure 1.1 shows a sketch of the solar wind - Earth interaction and the main boundaries.

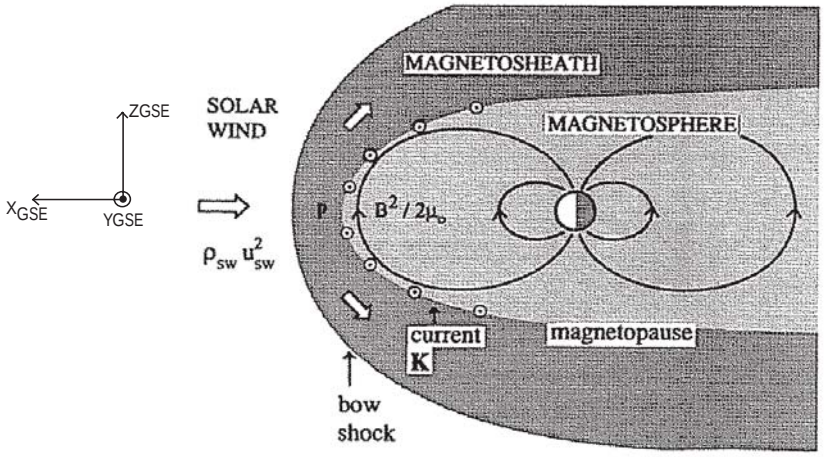

Figure 1.1: A sketch of the solar wind interaction with the Earth's magnetosphere. The Geocentric Solar Ecliptic (GSE) coordinate system is indicated. Adapted from [8].

The magnetopause is a surface whose location and shape are locally prescribed by the balance between solar wind and magnetospheric pressures. Across the magnetopause the magnetic field changes orientation and magnitude, thus the magnetopause is a current layer, as sketched in Fig. 1.2. Electrons and ions perform half a gyration around the magnetospheric field in opposite directions, thus producing a current. The thickness of the current sheet is approximately equal to the ion gyroradius.

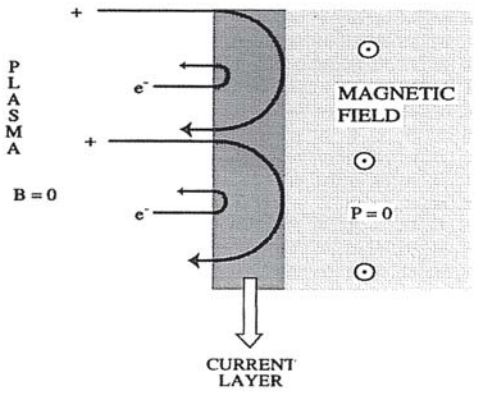

Figure 1.2: A sketch of the magnetopause current layer. From [8].

Chapter 2

Plasma transfer processes across the magnetopause

In normal conditions the magnetopause is an impenetrable boundary due to the frozen-in condition for both the solar and the magnetospheric plasmas. Though valid, this picture provides only a first-order approximation. There is in fact much evidence that solar wind plasma penetrates through the magnetopause. A magnetosheath-like plasma layer, the so-called *magnetospheric boundary layer*, is located on the magnetospheric side of the magnetopause. Also magnetospheric plasma has been observed outside the magnetopause in the *magnetosheath boundary layer*. Several processes have been proposed to explain this transfer of plasma across the magnetopause. The dominant process is considered to be *magnetic reconnection* between the interplanetary and terrestrial magnetic fields. This process will be introduced in this chapter. Other alternative processes are also briefly discussed. For more details refer to [33] and references therein.

2.1 Magnetic reconnection at the magnetopause

Transfer of mass, momentum and energy across the magnetopause can be explained by magnetic reconnection. During reconnection, the oppositely directed interplanetary and terrestrial frozen-in magnetic fields get in contact at the magnetopause in a very small region, the so-called *diffusion region*. There microscopic processes locally break down the frozen-in condition so that plasma and magnetic field can decouple while outside the diffusion region the magnetic field is still frozen-in. The result is that interplanetary and terrestrial magnetic field lines become interconnected and new 'reconnected' magnetic field lines are created. The mechanism is sketched in Fig. 2.1 where diffusion regions are gray shaded. Solar wind particles that initially move along blue field lines after this interconnection can move along reconnected red field lines and enter the magnetosphere. In the same way magnetospheric particles initially on green

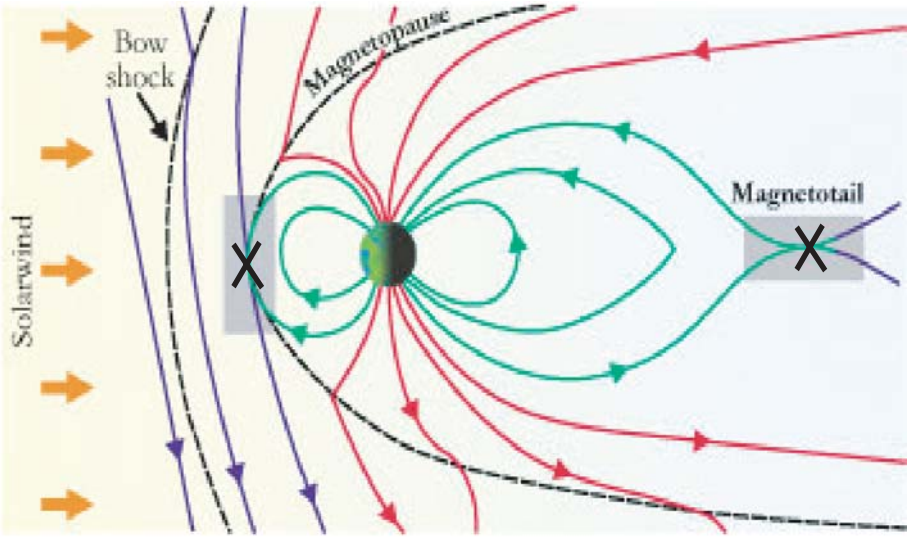

Figure 2.1: Magnetic reconnection in the magnetosphere. The locations where reconnection is initiated are indicated with two big X. Adapted from [11]

field lines can exit the magnetosphere along red lines. At the point where the fields interconnect, the *X-point* located in the center of the diffusion region, the plasma gains energy from the magnetic field. Magnetic field lines have in fact their own energy as it occurs in a rubber band. After the interconnection, the reconnected field lines are highly bent, as one can see in the red line close to the diffusion region in Fig. 2.1. As all systems in Nature, magnetic field lines prefer to have as minimum energy as possible so they will try to straighten thus releasing energy. This energy is gained by particles moving along field lines which get heated and accelerated. Once created at the X-point on the dayside magnetopause, the reconnected field lines are transported by the solar wind (from left to right in Fig. 2.1) towards the Earth's *magnetotail* where they eventually reconnect again.

Figure 2.2 is a sketch of the reconnection geometry close to the X-point for the case of two-dimensional (2D) and stationary reconnection at the subsolar magnetopause. The magnetopause (MP) is shown as a current layer with the magnetopause current I flowing out the plane containing the two reconnecting magnetic fields, often referred as the *reconnection plane*. This plane is perpendicular to the *magnetopause plane* that is the plane containing the magnetopause. At the subsolar point the reconnection plane is parallel to the XZ plane while the magnetopause plane is parallel to the YZ plane. In this 2D sketch the *magnetic separatrices*, the field lines connected to the X-point, are

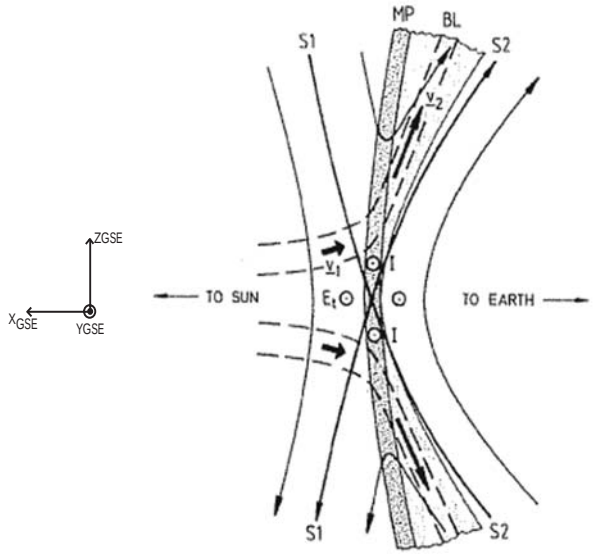

Figure 2.2: A 2D sketch of magnetic reconnection at the subsolar magnetopause for antiparallel magnetic fields. Adapted from [36]

indicated as $S1$ (outer separatrix) and $S2$ (inner separatrix). These field lines separate magnetic fields of different topologies, the interplanetary and the magnetospheric ones. The magnetospheric boundary layer (BL) is the layer of mixed magnetosheath and magnetospheric plasma located on the magnetospheric side of the magnetopause on the magnetospheric side.

In a 3D view the line connecting all the X-points on the magnetopause is called the *X-line* and the separatrices are surfaces. The X-line location in general depends on the orientation of the IMF. Figure 2.3 shows the X-line at the dayside magnetopause for a given IMF orientation. In the case of *component reconnection*, (a) in Fig. 2.3, the reconnecting magnetic fields are not antiparallel and the X-line is tilted with respect to the XY_{GSE} plane. For *antiparallel reconnection*, (b) in Fig. 2.3, half of the X-line is located in the Northern Emisphere and the other half in the Southern Emisphere on opposite sides.

Magnetic reconnection is an universal process occurring not only in the Earth's magnetosphere but also in laboratory plasmas, on the Sun and in the solar wind. Reconnection is considered to play an important role also in astrophysical plasmas, e.g. in stellar flares, accretion disks and astrophysical jets. This universality of magnetic reconnection is not surprising considering that 99% of the matter in the Universe is plasma and that magnetic fields are everywhere. In the next subsections we discuss definitions and models of reconnection.

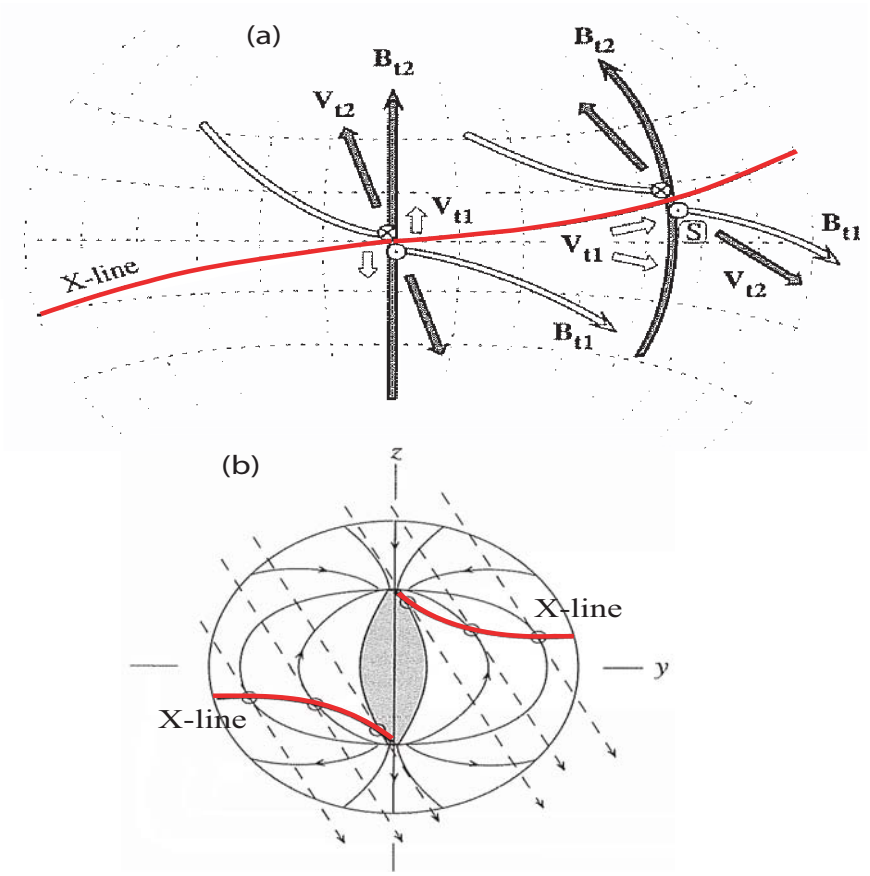

Figure 2.3: The X-line at the dayside magnetopause as seen from the Sun: (a) for component reconnection; subscripts 1, 2 refer to magnetosheath, magnetosphere respectively (adapted from [36]) and (b) for antiparallel reconnection (adapted from [9].

2.2 Definitions of magnetic reconnection

Magnetic reconnection has been studied for years both theoretically and observationally since it was first proposed in 1946 by Giovanelli [16] as a possible mechanism of particle acceleration in cosmic plasmas. In 1961 Dungey [13] applied this mechanism to magnetospheric physics. First direct evidence of magnetic reconnection at the Earth's magnetopause was found in 1979 by Paschmann [26]. Despite of many studies on reconnection, a commonly accepted definition of this mechanism has not been yet formulated and discussion is still ongoing. Here we briefly present possible definitions of magnetic reconnection. A more detailed discussion can be found in [29] and [21].

Magnetic reconnection is with no doubt a three-dimensional and time dependent plasma process. Nevertheless in some situations it can be a good approximation to describe it as a two-dimensional and stationary process. Although it is often objected that the two-dimensional picture is an oversimplified 'cartoon', the 2D stationary picture provides much physical insight and it is often consistent with observations. Nevertheless this description is sometimes not sufficient to explain the observations and a more general three-dimensional approach is required.

2.2.1 2D reconnection

Magnetic reconnection can be defined in 2D and steady-state conditions as a process having the following properties [29]:

1. it occurs at an X-point where two pairs of separatrices meet; during reconnection two magnetic field lines are brought towards the X-point; then they lie along the separatrices and are broken and reconnected
2. the electric field $\overrightarrow{E}$ is directed along the X-line thus perpendicularly to the reconnection plane
3. there is a change of magnetic connectivity of plasma elements due to the breaking of the frozen-in condition inside the diffusion region
4. there is a plasma flow across the separatrices

These properties of magnetic reconnection in 2D are shown in Fig. 2.4, part (a).

2.2.2 3D reconnection

A possible generalization of the magnetic reconnection definition in 3D can be obtained starting from point (2) in the 2D case. According to [32] and [18] *general magnetic reconnection* is a 'breakdown of magnetic connection due to a localized non-idealness'. This non-idealness is localized inside the diffusion region. A necessary and sufficient condition for its occurrence is:

$$\int E_{||} ds \neq 0 \tag{2.1}$$

where $E_{||}$ is the electric field parallel to the magnetic field and the integration is done along a field line *inside* the diffusion region. This is a very broad definition that would include processes usually not considered as magnetic reconnection like for example the presence of an $E_{||}$ above auroral arcs. More restrictive definitions of reconnection can be found in [29] and [21]. The general magnetic reconnection definition in 3D is illustrated in Fig. 2.4, part (b).

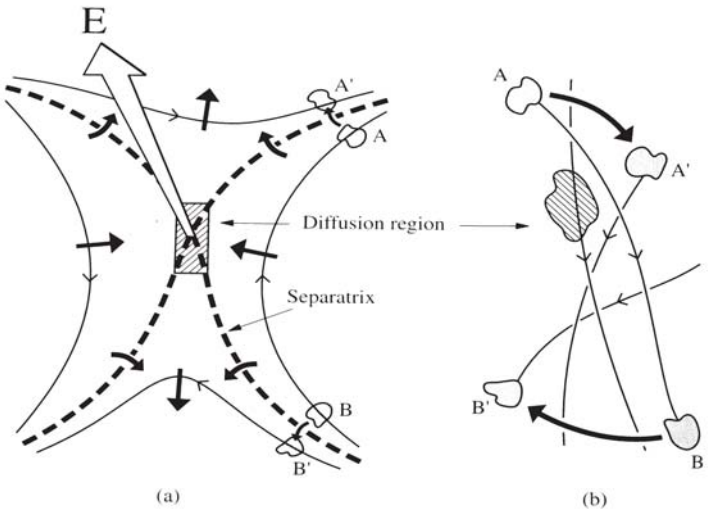

Figure 2.4: Properties of (a) 2D and (b) 3D magnetic reconnection. Plasma elements A and B initially connected by the same field line at later stage are no longer magnetically connected. From [29].

2.2.3 Our definition

The definitions of magnetic reconnection given above are either too restrictive or too wide. The 2D and steady-state definition is difficult to generalize in more general 3D and transient situations. On the other hand the general 3D definition given above would include too many phenomena and would be not useful on the observational point of view. We prefer to introduce our definition of magnetic reconnection that originates from the need to interpret observations in the magnetosphere. According to this definition magnetic reconnection is a process where:

1. the connectivity of magnetic field lines changes:
   (a) there is a parallel electric field in the diffusion region
   (b) $B_N \neq 0$ at the current sheet
2. there is a transport across the boundary:
   (a) particles are transmitted across the current sheet in both directions
3. energy is converted from the magnetic field to the plasma:
   (a) plasma jets are observed in the current sheet/boundary layer
   (b) there is a substantial plasma heating

4. particle are accelerated to high energies:
   (a) there are strong electric fields
   (b) there are strong currents

2.3 Models of magnetic reconnection

Many models of magnetic reconnection have been proposed, see [29] for a detailed discussion. In this section we limit to describe the two-dimensional and steady-state models by Sweet and Parker [25, 37] and by Petschek [27], together with a generalization of Petschek's model for the magnetopause by Levy [20]. Before starting to describe the different models, we briefly recall some basic equations. Refer to [5] and [30] for a more complete treatment.

2.3.1 Basic equations

A useful framework to describe magnetic reconnection is the magnetohydrodynamic (MHD) approximation. In MHD the plasma is described as conductive fluid in electric and magnetic fields. No distinction is done between the dynamics of ions and electrons. The MHD approximation is valid for scales larger than one ion gyroradius that is also the typical thickness of the current sheet.
In presence of a finite plasma conductivity σ the equation describing the magnetic field $\overrightarrow{B}$ is the *induction equation*:

$$\frac{\partial \overrightarrow{B}}{\partial t} = \nabla \times (\overrightarrow{u} \times \overrightarrow{B}) + \frac{1}{\mu_0 \sigma} \nabla^2 \overrightarrow{B} \tag{2.2}$$

where $\overrightarrow{u}$ is the plasma velocity and μ_0 the vacuum permeability. The first term on the right hand side of Eq. 2.2 is called the *convective* term while the second one the *diffusive* term. The ratio (in order of magnititude) between the convective term and the diffusive term is the *magnetic Reynolds number*:

$$R_m = \mu_0 \sigma L_* U_* \tag{2.3}$$

where L_* and U_* are typical length and velocity of the system.
The electric field is given by:

$$\overrightarrow{E} + \overrightarrow{u} \times \overrightarrow{B} = \frac{\overrightarrow{J}}{\sigma} \tag{2.4}$$

where $\overrightarrow{J}$ is the current. The other governing equations for the plasma are the *continuity equation*:

$$\frac{\partial \rho}{\partial t} + \nabla \cdot (\rho \overrightarrow{u}) = 0 \tag{2.5}$$

and the equation of motion:

$$\frac{\partial \overrightarrow{u}}{\partial t} + (\overrightarrow{u} \cdot \nabla) \overrightarrow{u} = -\frac{\nabla p}{\rho} + \frac{\overrightarrow{J} \times \overrightarrow{B}}{\rho} \tag{2.6}$$

where ρ is the mass plasma density and p the plasma pressure.
In absence of collisions, the conductivity σ is infinite and the electric field is given by:

$$\overrightarrow{E} + \overrightarrow{u} \times \overrightarrow{B} = 0 \tag{2.7}$$

This regime is called *ideal MHD* and it corresponds to the situation where the magnetic field is frozen into the plasma. In ideal MHD conditions Eq. 2.2 reduces to:

$$\frac{\partial \overrightarrow{B}}{\partial t} = \nabla \times (\overrightarrow{u} \times \overrightarrow{B}) \tag{2.8}$$

and $R_m >> 1$.

2.3.2 Sweet-Parker reconnection

A sketch of a 2D and steady-state reconnection geometry according to Sweet-Parker model is shown in Fig. 2.5, top part. The figure shows the reconnection plane XZ with the antiparallel reconnecting magnetic fields in Z direction and the normal to the current sheet in X direction. The system has size $2L$ along the current sheet (Z direction) and $2a$ across the current sheet (X direction). The magnetic field vanishes at the center.

We now describe the basics of the Sweet-Parker model following the derivation by [29]. In the inflow region the electric field is given by:

$$E = u_0 B_0 \tag{2.9}$$

At the center of the diffusion region where the magnetic field is zero the electric field is:

$$E = \frac{J}{\sigma} \tag{2.10}$$

The current can be obtained applying Ampère's law across the current sheet:

$$J = \frac{B_0}{\mu_0 a} \tag{2.11}$$

In steady-state the electric field is constant so that combining Eq. 2.9, Eq. 2.10 and Eq. 2.11 we get the relation:

$$u_0 = \frac{1}{\mu_0 \sigma a} \tag{2.12}$$

Integration the continuity equation 2.5 over the diffusion region we get:

$$L u_0 = a u_e \tag{2.13}$$

where u_e is the outflow speed. Then eliminating the width a between Eq. 2.12 and Eq. 2.13 we get:

$$u_0^2 = \frac{u_e}{\mu_0 \sigma L} \tag{2.14}$$

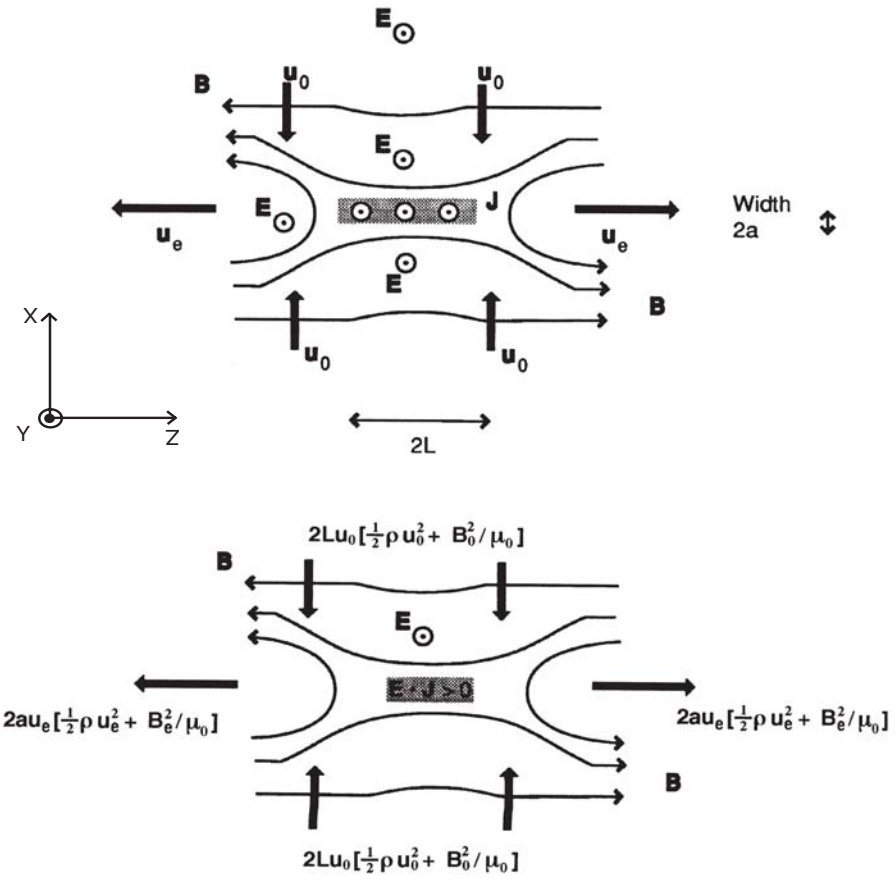

Figure 2.5: Top: schematic of 2D steady-state reconnection according to Sweet-Parker model. The shaded region with length $2L$ and width $2a$ is the diffusion region. Bottom: energy balance in the Sweet-Parker model. Energy input and outflow rates are indicated. Adapted from [8].

In dimensionless variables Eq. 2.14 can be written as:

$$M_0 = \frac{\sqrt{\frac{u_e}{u_{A0}}}}{\sqrt{R_{m0}}} \tag{2.15}$$

where

$$M_0 = \frac{u_0}{u_{A0}} \tag{2.16}$$

is the *inflow Alfvén Mach number* or *dimensionless reconnection rate* and

$$R_{m0} = L u_{A0} \sigma \mu_0 \tag{2.17}$$

is the magnetic Reynolds number based on the inflow Alfvén speed $u_{A0} = \frac{B_0}{\sqrt{\mu_0 \rho}}$ with ρ plasma density.
Once u_e and therefore u_0 from Eq. 2.14 are known for a given L then Eq. 2.13 determines the width a as:

$$a = L\frac{u_0}{u_e} \tag{2.18}$$

The outflow magnetic field strength is obtained by magnetic flux conservation as:

$$B_e = B_0\frac{u_0}{u_e} \tag{2.19}$$

To obtain the outflow speed u_e we need to consider the equation of motion 2.6. If we neglect the effect of thermal pressure and consider steady-state situation then the Lorentz force $(\overrightarrow{J} \times \overrightarrow{B})_z$ is the force that accelerates the plasma from rest to u_e over the distance L along the current sheet. Imposing balance between the Lorentz force and the inertial term $\rho(\overrightarrow{u} \cdot \nabla)u_z$ we get:

$$\rho\frac{u_e^2}{L} \approx \frac{B_0 B_e}{\mu_0 a} \tag{2.20}$$

Combining Eq. 2.20 with Eq. 2.13 and Eq. 2.19 we finally get the important result:

$$u_e = \frac{B_0}{\mu_0 \rho} = u_{A0} \tag{2.21}$$

that means that the magnetic force accelerates the plasma to the Alfvén speed. The magnetic field therefore reconnects at the speed given by:

$$u_0 = \frac{u_{A0}}{\sqrt{R_{m0}}} \tag{2.22}$$

Due to the large value of the magnetic Reynolds number $R_{m0} >> 1$ we have $u_0 << u_{A0}$, $B_e << B_0$ and also $a << L$.
It is interesting to consider the energy balance in the Sweet-Parker reconnection shown in Fig. 2.5, bottom part. The inflow rate of electromagnetic (EM) energy is the flux of the Poynting vector $\overrightarrow{S} = \frac{\overrightarrow{E} \times \overrightarrow{B}}{\mu_0}$ through the inflow region:

$$\Phi(\overrightarrow{S}) = E\frac{B_0}{\mu_0}L = \frac{u_0 B_0^2 L}{\mu_0} \tag{2.23}$$

The ratio between the inflow rate of kinetic (K) energy and the inflow rate of EM energy is then:

$$\frac{(K)_0}{(EM)_0} = \frac{(1/2)\rho u_0^2}{B_0^2/\mu_0} = \frac{u_0^2}{2u_{A0}^2} << 1 \tag{2.24}$$

i.e. most of the inflowing energy is magnetic. Because of the condition $a << L$ and $B_e << B_0$, the outflow rate of EM energy $E\frac{B_e}{\mu_0}a$ is much smaller than the inflow rate of EM energy. This means that in the reconnection process magnetic

energy must be dissipated. The ratio between the outflow rate of K energy and the inflow rate of EM energy is:

$$\frac{(K)_e}{(EM)_0} = \frac{(1/2)\rho u_e^2 (u_e a)}{u_0 B_0^2 L/\mu_0} = \frac{(1/2)u_e^2}{u_{A0}^2} = \frac{1}{2} \tag{2.25}$$

showing that half of the inflow magnetic energy is converted to plasma kinetic energy and half to thermal energy. Thus the effect of reconnection is to create hot and fast plasma jets.

2.3.3 Petschek and Levy reconnection

In Sweet-Parker reconnection the size of the system equals the size of the diffusion region and all the plasma must go through the diffusion region. As a consequence the reconnection rate estimated from Eq. 2.16 is quite small and not consistent with observations e.g. of solar flares. In Petschek reconnection the Sweet-Parker diffusion region is replaced by a much smaller diffusion region extending into two standing slow-shocks in the outflow region, as shown in Fig. 2.6. With this configuration only a small fraction of the inflowing plasma must

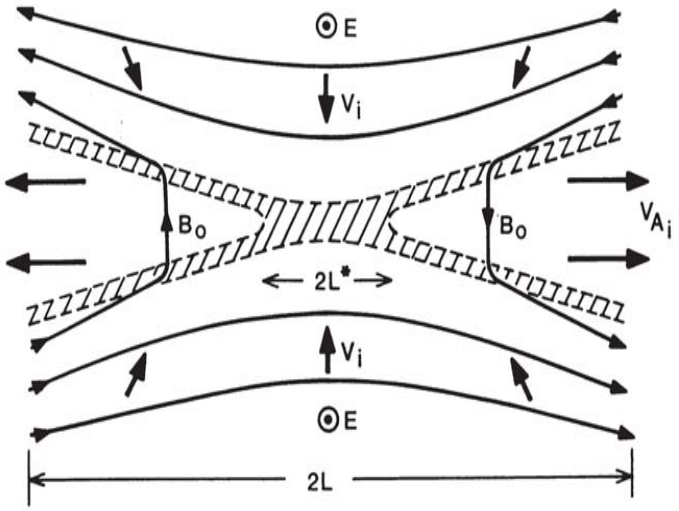

Figure 2.6: Schematic of 2D steady-state reconnection according to Petschek model. The size of the diffusion region is $2L^*$ while the size of the system is $2L$. The diffusion region bifurcates into two standing slow-shocks in the downstream flow. Current-carrying regions are shown hatched. From [6].

go through the diffusion region while the most part of it is accelerated at the slow-shocks away from the diffusion region. As a result reconnection can proceed much faster than in the Sweet-Parker model and more realistic reconnection rates are obtained.

The Petschek's model describes symmetric reconnection where the two inflow regions have the same properties. Although this situation is suitable for tail reconnection, at the magnetopause the two inflowing regions are usually quite different. In the Levy model [20] shown in Fig. 2.7 plasma is inflowing mainly in one direction (magnetosheath side). In the inflow region the density is much higher than on the other side (magnetospheric side) but the magnetic field strength is much smaller. As a result of this configuration the slow-shocks in Petschek model are substituted by a *rotational discontinuity* and a standing *slow expansion wave*. Across the rotational discontinuity the magnetic field changes its orientation from magnetosheath to magnetospheric direction keeping constant strength. Also the density stays constant. In this layer plasma jets are observed, as we will discuss in section 4.1.1. Across the slow wave the strength of the magnetic field and the density change gradually to match their values on the magnetospheric side. At the magnetopause the rotational discontinuity corresponds to the current sheet while the slow wave to the magnetospheric boundary layer.

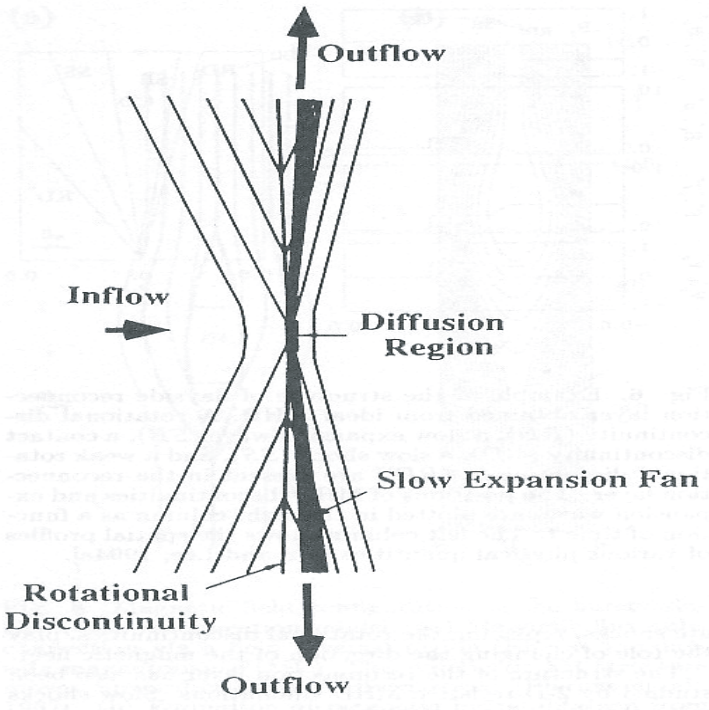

Figure 2.7: Schematic of 2D steady-state reconnection according to Levy's model at the magnetopause. From [19].

2.4 Alternative mechanisms

Several mechanisms alternative to magnetic reconnection have been proposed to explain the transfer of mass, momentum and energy across the magnetopause. In this section we briefly discuss some of these mechanisms. They are sketched in Fig. 2.8. See [33] and [40] for more details.

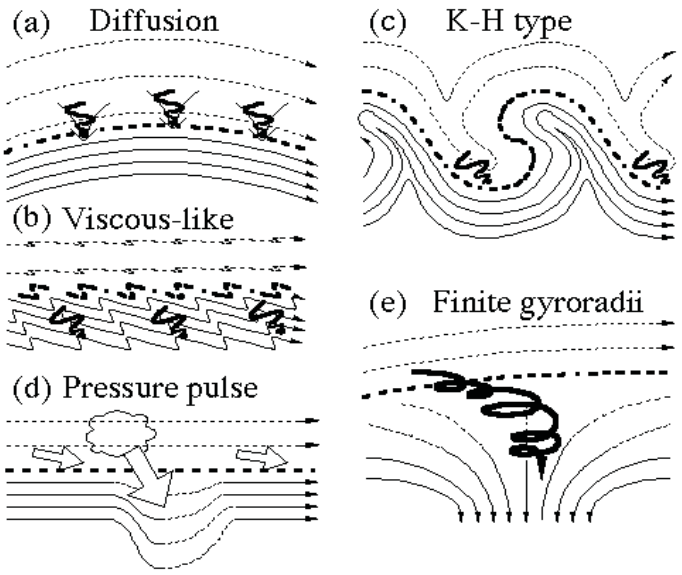

Figure 2.8: Non-reconnection plasma transfer mechanisms across the magnetopause. Adapted from [40].

During *diffusion* plasma diffuses transversally to the magnetic field according to the ordinary diffusion equation:

$$\frac{\partial n}{\partial t} = D\nabla^2 n \tag{2.26}$$

where n is the plasma density and D the *diffusion coefficient*. This process requires a distortion of the particle motion due to a localized particle scattering. In collisionless plasmas like the solar wind and the magnetospheric plasmas, this scattering is provided by anomalous collisions due to wave-particle interactions. Evidence of diffusion at the magnetopause is controversial, e.g. it is not completely established what is the minimum diffusion coefficient D necessary to explain the thickness of the observed magnetospheric boundary layer. Also it is not yet clear which wave modes can account for the required anomalous collisions. Diffusion could play an important role when reconnection is less efficient, for example when the interplanetary magnetic field is pointing in northward direction.

The *viscous-like* mechanism [4] invokes the creation of a viscous boundary layer between the solar wind and magnetospheric plasma where momentum and energy can be transferred by sound waves. No evidence of this mechanism have been reported in observations.

The *Kelvin-Helmholtz* (KH) instability at the magnetopause has also been invoked as possible transfer process. The KH instability develops at the magnetopause in the form of large surface waves that can transport energy and momentum from the magnetosheath into the magnetospheric boundary layer. In a non-linear stage the instability could produce large-scale eddies relatively deep inside the boundary layer that could be responsible also for mass transfer, as supported by recent observations of macroscopic vortexes at the magnetopause by [17].

The *impulsive penetration* mechanism is based on the idea that plasma can be transferred across the magnetopause via 'blobs' of magnetosheath plasma with excess momentum. After the penetration, these blobs become embedded in the less dense magnetospheric plasma on closed field lines. Recent evidence of impulsive penetration at the magnetopause has been provided by [22].

Finally *finite gyroradius* effects have also been invoked to explain plasma transfer. In this mechanism energetic magnetosheath and magnetospheric particles are able to cross the magnetopause because their gyroradii are larger than the magnetopause thickness. This can occur especially in regions of weak magnetic field.

Chapter 3

The Cluster mission

The European Space Agency cornerstone Cluster mission [14] is the first magnetospheric mission with four identical spacecraft.

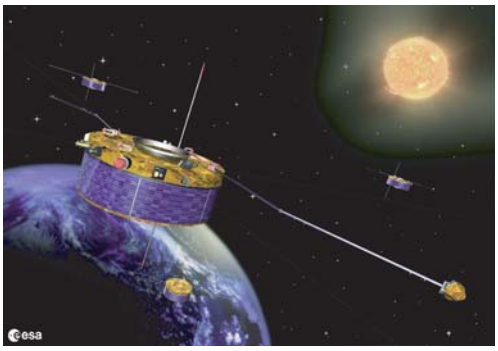

Figure 3.1: Artist's impression of the Cluster spacecraft. From [3].

The spacecraft move along their orbit in a tetrahedrical configuration with variable inter-spacecraft separation, thus allowing the study of structures such as magnetospheric boundaries at different spatial scales. A sketch of Cluster orbit is shown in Fig. 3.2 while the main Cluster parameters are shown in Table 3.1.

Inclination	90°
Perigee-Apogee	4-19.6 R_E
Orbital period	57h
Spin period	4s
Spin axis direction	Ecliptic north pole

Table 3.1: Main Cluster parameters.

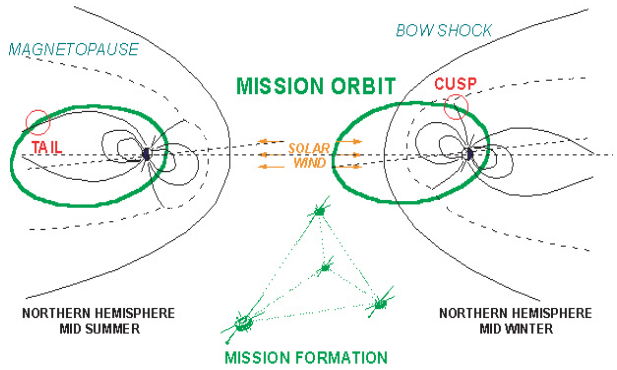

Figure 3.2: Cluster orbits in two different periods of the year. From [2].

Each spacecraft is equipped with the same set of eleven instruments that can simultaneously measure plasma quantities and electromagnetic fields at four different points in space, thus allowing the first three-dimensional study of the Earth's magnetosphere and its surrounding boundaries. A brief description of Cluster instruments is shown in Table 3.2.

Acronym	Experiment	Country
ASPOC	Active Spacecraft Potential Control	Austria
CIS	Cluster Ion Spectrometry	France
EDI	Electron Drift Instrument	Germany
FGM	Fluxgate Magnetometer	U.K.
PEACE	Plasma Electron and Current Experiment	U.K.
RAPID	Research with Adaptive Particle Imaging Detectors	Germany
DWP	Digital Wave Processing Experiment	U.K.
EFW	Electric Field and Waves	Sweden
STAFF	Spatio-Temporal Analysis of Field Fluctuations	France
WBD	Wide Band Data	U.S.A
WHISPER	Waves of High Frequency and Sounder for Probing of the Electron Density by Relaxation	France

Table 3.2: The Cluster Experiments. Adapted from [10]

Chapter 4

Observations of magnetic reconnection at the Earth's magnetopause

The Earth's magnetosphere is the best laboratory to study magnetic reconnection. In the magnetosphere in fact it is possible to fly one or more spacecraft and measure in-situ plasma and electromagnetic field quantities over a large number of characteristic temporal and spatial scales. Magnetic reconnection occurs in the magnetosphere in two key regions: the magnetopause and the magnetotail, as shown in Fig. 2.1. We concentrate in this chapter on the main observational properties of reconnection at the magnetopause both at large and at small scales.

4.1 Large scales

At scales larger than one ion gyroradius, that is roughly the thickness of magnetopause current layer, MHD is a valid approximation as discussed in 2.3.1. In MHD approximation the magnetopause can be described as a *MHD discontinuity* [5]. Figure 4.1 shows two cases of MHD discontinuities. In absence of reconnection the magnetopause can be described as a *tangential discontinuity*, case (b) in Fig. 4.1. A tangential discontinuity is a boundary where the tangential components of the magnetic field $\overrightarrow{B}_t$ and of the plasma velocity $\overrightarrow{u}_t$ change arbitrarily in direction and strength. Both the magnetic field and the plasma velocity components perpendicular to the magnetopause, B_n and u_n, are zero and there is neither mass nor magnetic flux flow across the boundary. Across a rotational discontinuity there is instead a finite mass and magnetic flux flow. The normal components B_n and u_n are different from zero and constant across

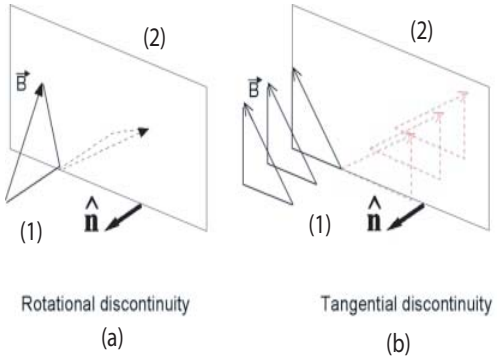

Figure 4.1: Two MHD discontinuities: (a) rotational and (b) tangential. Adapted from [1].

the boundary and they satisfy the following relation:

$$u_n = \pm \frac{B_n}{\sqrt{\mu_0 \varrho}} \tag{4.1}$$

where the velocity u_n is measured in the discontinuity reference frame. The tangential components of the magnetic field $\overrightarrow{B}_t$ and of the plasma velocity $\overrightarrow{u}_t$ change across the boundary according to the *Walén relation*:

$$\triangle \overrightarrow{u}_t = \pm \frac{\triangle \overrightarrow{B}_t}{\sqrt{\mu_0 \varrho}} \tag{4.2}$$

where $\triangle$ denotes the difference between quantities on the two sides of the boundary. For the more general case of anisotropic plasma Eq. 4.2 can be written as:

$$\overrightarrow{u}_{t2} - \overrightarrow{u}_{t1} = \pm (\frac{1-\alpha_1}{\mu_0 \varrho_1})^{1/2} [\overrightarrow{B}_{t2} (\frac{1-\alpha_2}{1-\alpha_1}) - \overrightarrow{B}_{t1}] \tag{4.3}$$

where $\alpha = \frac{\mu_0 (p_\parallel - p_\perp)}{B^2}$ is the *pressure anisotropy* and $\parallel$,$\perp$ refer to directions parallel and perpendicular to the magnetic field respectively. The subscripts $1, 2$ indicate quantities on the two sides of the discontinuity.

4.1.1 Fluid evidence

When reconnection is active, the magnetopause boundary can be described as a rotational discontinuity. The following relations then must hold:

$$B_n \neq 0 \tag{4.4}$$

$$u_n \neq 0 \tag{4.5}$$

$$|\overrightarrow{E}_t| \neq 0 \tag{4.6}$$

providing evidence of ongoing reconnection and a measurement of the reconnection rate:

$$M_n = \frac{u_n}{u_A} = \frac{B_n}{|\overrightarrow{B}|} \tag{4.7}$$

where u_A is the Alfvén velocity calculated in the inflow region. Unfortunately a direct measurement of B_n, u_n and $|\overrightarrow{E}_t|$ at the magnetopause is quite difficult because they are usually small compared to measurement uncertainties, as discussed in [33] and references therein. The tangential quantities instead do not usually suffer this limitation. *Fluid evidence* of reconnection can be obtained verifying the *tangential stress balance* prescribed by Eq. 4.3 across the magnetopause. Eq. 4.3 is evaluated between one *magnetosheath reference level*, point 1 in Fig. 4.2, and one interval inside the accelerated plasma jet in the magnetopause/magnetospheric boundary layer, point 2 in Fig. 4.2. The signs $+,-$ in Eq. 4.3 correspond to $B_n < 0, B_n > 0$ respectively that is to observations northward, southward of the X-point. When Eq. 4.3 is satisfied then the magnetopause is locally a rotational discontinuity thus providing evidence of ongoing reconnection. This test is called *Walén test* [26, 36].

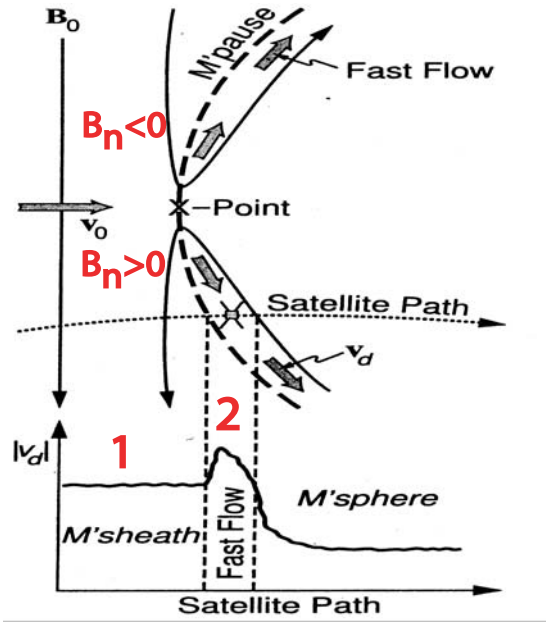

Figure 4.2: A sketch of plasma jets at the magnetopause. Adapted from [38].

Another equivalent method to test the tangential stress balance across the magnetopause is to perform the Walén test in the *deHoffmann-Teller frame* [34, 35]. If $B_n \neq 0$ across the magnetopause then magnetic field lines on both sides of the boundary must move together. Then it must exist an inertial reference frame where the flows are aligned with the magnetic field and the electric field vanishes on both sides of the boundary. This reference frame is called the *deHoffmann-Teller (HT) frame* [12]. The HT frames slides along the magnetopause at the 'field-line velocity' $\overrightarrow{U}_{HT}$ that is the velocity at which the reconnected field lines move along the magnetopause. The component of $\overrightarrow{U}_{HT}$ along the normal to the magnetopause $\widehat{n}$ is the velocity of the magnetopause in its normal direction $U_{MP} = \overrightarrow{U}_{HT} \cdot \widehat{n}$. The existence of a proper HT frame is thus a necessary (but not sufficient) condition for an open magnetopause and ongoing reconnection. In the HT frame the Walén test becomes a verification of the relation:

$$\overrightarrow{U} - \overrightarrow{U}_{HT} = \pm \overrightarrow{U}_A \tag{4.8}$$

where $\overrightarrow{U}_A$ is the local Alfvén velocity. An example of successful Walén test in the deHoffmann-Teller frame is shown in Fig. 4.3. That the test is successful is indicated by a slope close to unit in Fig. 4.3, panel (b). A positive/negative slope corresponds to $+/-$ sign in Eq. 4.3 that is $B_n < 0/B_n > 0$.

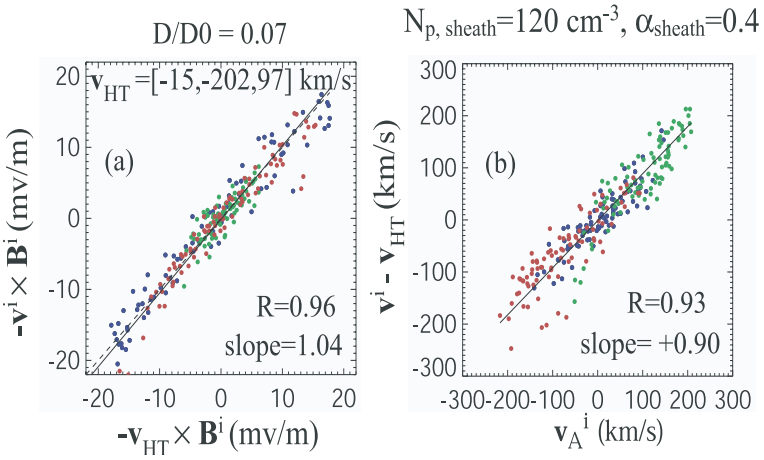

Figure 4.3: An example of Walén test in the deHoffmann-Teller frame. Panel (a) shows that it exists a proper HT frame while panel (b) shows the successful Walén test. From [28].

Evidence of reconnection discussed so far has been presented under the assumption of steady-state. There is much evidence that reconnection proceeds also in a transient fashion [31]. According to this mechanism isolated flux tubes reconnect at the magnetopause as shown in Fig. 4.4 generating so-called *flux transfer events*(FTE). Typical evidence of an FTE at the magnetopause is a bipolar B_n signature together with plasma jets observed during magnetopause crossing.

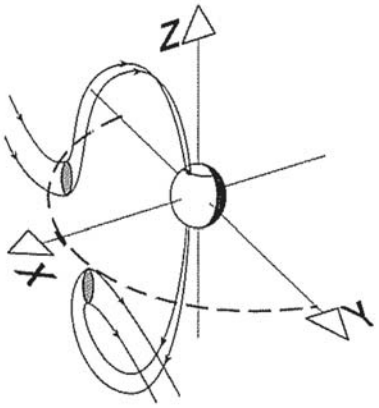

Figure 4.4: A sketch of an FTE. Adapted from [29]

4.1.2 Kinetic evidence

An independent and complementary evidence of reconnection can be obtained considering the motion of particles around the reconnection region. Quantitative evidence can be obtained from the analysis of particle motion in the HT frame [7]. The acceleration of a particle in the current sheet is described in Fig. 4.5 where the motion of the particle is sketched both in the Earth's frame and in the HT frame. In the Earth's frame, part (a) in Fig. 4.5, the particle inflowing along a reconnected field line from the left has both a parallel velocity $u_{\|i}$ and perpendicular velocity u_{E1} due to $\overrightarrow{E} \times \overrightarrow{B}$ motion. In HT frame where $\overrightarrow{E} = 0$ on both sides of the magnetopause, the particle has only a parallel velocity $u_{\|i} + u_{HT}$. In the HT frame only particles with positive velocity are transmitted across the magnetopause implying that in the Earth's frame transmitted particle must have velocity $|u_{\|i}| > |u_{HT}|$. This situation is shown in Fig. 4.5 part (d) where a cut of the ion distribution function just inside the magnetopause is shown in the magnetopause plane. As one can see in the figure, the transmitted magnetosheath ions show a typical low-energy cut-off at a parallel velocity equal to u_{HT}. These distribution functions are often called 'D-shaped' distribution

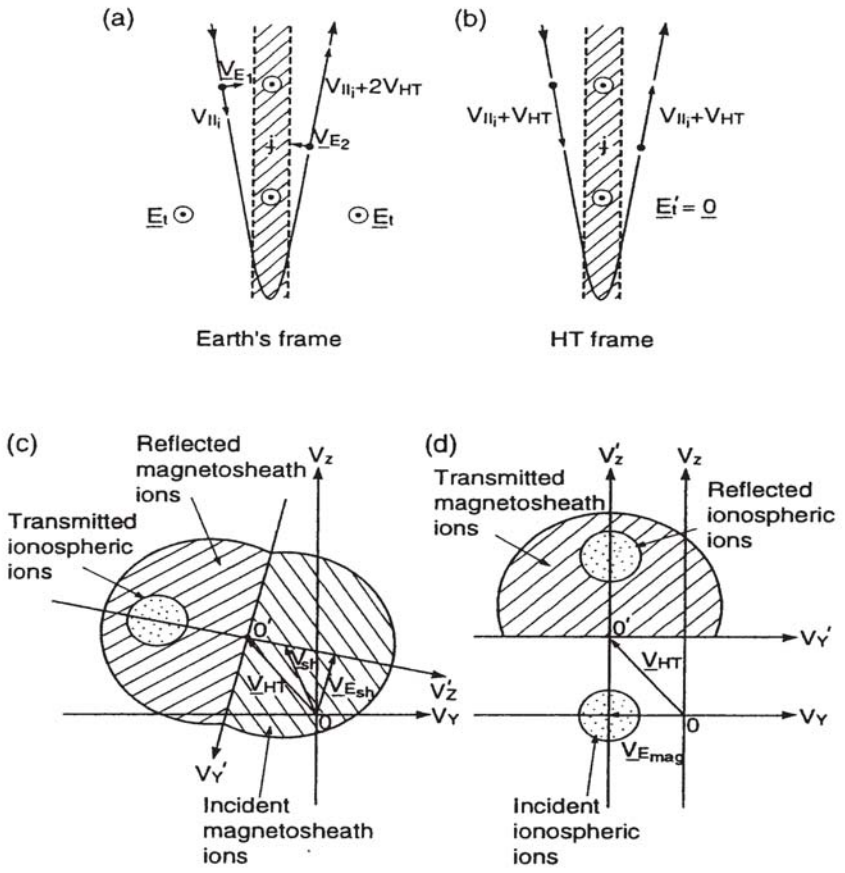

Figure 4.5: Behavior of a particle transmitted across the magnetopause in (a) Earth's reference frame and (b) HT frame. The bottom sketches show ion velocity distribution functions in the magnetopause plane (c) just outside the magnetopause on magnetosheath side and (d) just inside the magnetopause on the magnetospheric side. From [7].

functions. A similar constraint for the velocity of reflected particles can also be obtained, see [7] for more details.

Figure 4.6 shows an example of an observed D-shaped distribution function for transmitted magnetosheath ions inside the magnetopause.

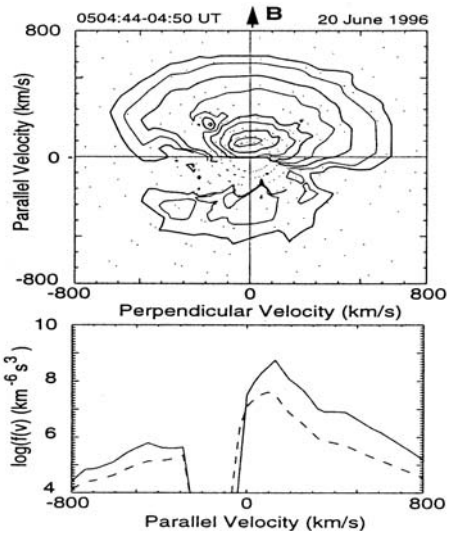

Figure 4.6: Observed D-shaped ion distribution function. From [15].

4.2 Small scales

In the diffusion region the MHD treatment is no longer valid. We consider separately the contribution of electrons and ions in the *two fluid theory* [29]. The electric field can then be written as:

$$\overrightarrow{E} = -\overrightarrow{u} \times \overrightarrow{B} + \frac{\overrightarrow{J}}{\sigma} + \frac{m_e}{ne^2}[\frac{\partial \overrightarrow{J}}{\partial t} + \nabla \cdot (\overrightarrow{u}\overrightarrow{J} + \overrightarrow{J}\overrightarrow{u}] - \frac{\overrightarrow{J} \times \overrightarrow{B}}{ne} - \frac{\nabla \cdot \mathbf{P}_e}{ne} \quad (4.9)$$

where $\overrightarrow{u}$ is the ion velocity, n the plasma density (quasi neutrality is assumed), $\overrightarrow{J}$ the current and $\mathbf{P}_e$ the electron pressure tensor. The first two terms on the right-hand side of Eq. 4.9 are the same as in MHD. The third term is the *electron inertial term* describing electron inertia effects, the fourth the so-called *Hall term* and the last one the *electron pressure term* describing effects due to electron pressure gradients. The relative importance of these terms is related to different characteristic length scales, see [33] and references therein for a complete discussion.

At spatial scales $\sim \lambda_i$, where $\lambda_i = \frac{c}{\omega_{pi}}$ is the *ion inertial length* and ω_{pi} the ion plasma frequency, the ion motion is decoupled from the magnetic field inside the *ion diffusion region*, as shown in Fig. 4.7. The magnetic field is still frozen in the electron fluid. In the ion diffusion region the electric field is balanced by the Hall term and there are a quadrupolar out-of-plane magnetic field (Hall B_y in Fig. 4.7) and a bipolar electric field (Hall E_x in Fig. 4.7) as shown at the magnetopause e.g. by [23] and [39].

At smaller scales $\sim \lambda_e$, where $\sim \lambda_e = \frac{c}{\omega_{pe}}$ is the *electron inertial length* and ω_{pe} is the electron plasma frequency, also the electrons decouple from the magnetic field inside the *electron diffusion region*, as shown in Fig. 4.7. It is not still clear which term in Eq. 4.9 is responsible for decoupling the electrons from the magnetic field though the electron pressure term is thought to play a major role [24].

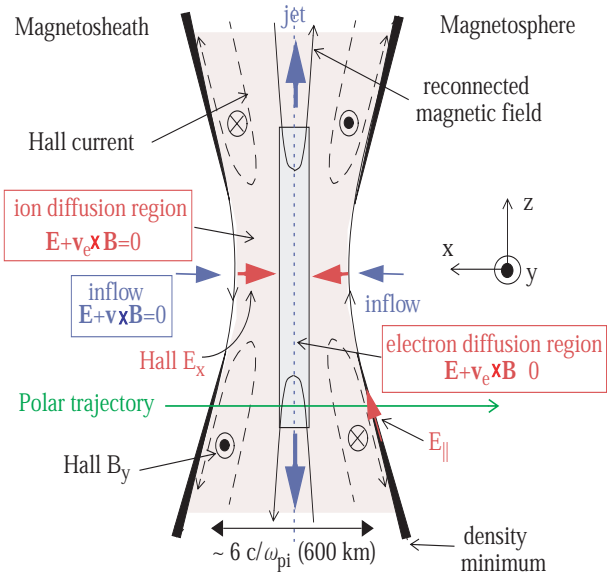

Figure 4.7: A sketch of the ion and electron diffusion regions. The separatrices are also shown extending away from the diffusion regions. Density minima and parallel electric fields $E_\|$ are located along the separatrices. From [23].

Chapter 5

Summary of papers

The work done in this thesis contributes to the study of magnetic reconnection in the magnetosphere. Among many ways to 'attack' the problem, we have preferred to concentrate on the multi-scale aspect of reconnection. Magnetic reconnection is in fact fast initiated at microscopic scales but affects very large volumes in space over long time. Therefore it is a key point to study reconnection at different spatial and temporal scales. A great opportunity to perform this study is given by Cluster spacecraft observations in the magnetosphere. First of all, the Earth's magnetosphere is the best laboratory to study magnetic reconnection at different scales. In the magnetosphere in fact the resolution of instruments onboard spacecraft can cover most of temporal and spatial scales related to magnetic reconnection and perform in-situ measurements of plasma and electromagnetic fields parameters. This cannot be done in the same detail in other environments where reconnection occurs such as laboratory, solar or astrophysical plasmas. Furthermore with Cluster we have for the first time four simultaneous points of observation that allow to distinguish temporal from spatial variations. In this framework we have been able to improve the understanding of reconnection processes based on observations at the Earth's magnetopause.

In **Paper I** we study magnetic reconnection at large temporal (several hours) and spatial (several Earth's radii) scales. We report multi-spacecraft Cluster observations of magnetic reconnection at the high-latitude magnetopause under northward interplanetary magnetic field. We concentrate on one event occurring on December 3, 2001 when the Cluster spacecraft were skimming the magnetopause for several hours. The orbit and configuration of the spacecraft were such that at least one satellite was present in the magnetopause/boundary layer during most of the time. We present fluid and kinetic evidence of magnetic reconnection. Our observations are consistent with magnetic reconnection occurring tailward of the cusp and going on continuously for a period of about four hours. The observed directions of the reconnection flows agree with the IMF orientation and this indicates that reconnection is globally controlled by

the interplanetary magnetic field. In a few cases we observe ion jet reversals that indicate possible spacecraft crossings close to the X-line. The observation of low magnetic shear across the magnetopause during a jet reversal is consistent with component merging at least in one case.
In summary, we have established in Paper I that the magnetopause is not a perfect shield against the solar wind and that magnetic reconnection indeed creates 'holes' at the magnetopause. Once created, these holes seem to stay open for long time. Also, the locations on the magnetopause where they form is directly determined by the orientation of the interplanetary magnetic field. The holes do not necessarily form where the reconnecting magnetic fields are exactly antiparallel, as expected from some theories, but also for other orientations of the magnetic fields. This means that the size of these holes on the magnetopause can be larger than when antiparallel fields reconnect.

Once established the general properties of reconnection at the large scales, we concentrate in **Paper II** on observations at smaller scales and study the microphysics of magnetic reconnection. We analyze a short time interval of data from the same event studied in Paper I. This time we can use data only from one spacecraft due to the large spacecraft separation. We interpret one ion jet reversal, from sunward to tailward direction, as an indication of a passage close to the X-line. We identify the main regions around the X-line and we compare them with a numerical simulation of reconnection, finding a good agreement. From the comparison we estimate a distance from the X-line of about 3000 km that corresponds to 60 ion inertial lengths. We concentrate on one region in particular, the separatrix region on the magnetospheric side of the magnetopause. The separatrix region is located between the magnetic separatrix, i.e. the magnetic field line connected to the X-line, and the tailward reconnection jet. The separatrix region has a width of several ion inertial lengths and it contains subregions with widths of about an ion inertial length. These subregions are highly structured in the electric field down to Debye length scales. As an example, electrostatic solitary waves are observed at the boundary between the separatrix region and the reconnection jet and inside the reconnection jet. Such waves are not observed within the separatrix region itself. Inside the separatrix region we obtain for the first time simultaneous high-time resolution measurements of electric field spectra and electron distribution functions. This allows a detailed study of wave-particle interactions there. As a result we find that one subregion, a density cavity observed adjacent to the separatrix, has strong DC electric fields, electron beams accelerated away from the X-line and intense wave turbulence around both the plasma frequency and the lower hybrid frequency. In the density cavity, as well as in another subregion, lower hybrid waves can be important for plasma transport across as the anomalous collision frequency estimated from electric field fluctuations is of the order of the local lower hybrid frequency. We speculate that this transport could be important not only across a few subregions but even across the entire separatrix region. The comparison of these observations at small scales with numerical simulations shows generally agreement even though some features are not resolved by the simulations.

In summary, we have studied in Paper II the details of what is happening around one of the holes created by reconnection at the magnetopause. We have established that there is much action along the magnetic field lines connected to that hole, the separatrix regions, even when we look a little bit far away from it. Our results suggest that much information about the microphysics of those holes can be obtained from studying the separatrix regions.

Chapter 6

Future work

A few specific suggestions for future work come directly from the results presented in this thesis:

- Magnetic reconnection is a continuous process in time though rather dynamic. This result comes from the observations of reconnection signatures for many hours. Is this also true at short time scales? Or instead reconnection proceeds in intermittent way, switching on-off at short time scales $\sim$ 1s or less? This issue is possibly related to the observations of micro-FTEs like those found in Paper II. To conclusively relate such structures to the modulation of the reconnection rate we need other events with more than one spacecraft.

- Magnetic reconnection at the magnetopause does not require antiparallel magnetic fields. This also agree with recent numerical simulations. Is then antiparallel reconnection just a special case at the magnetopause? To unambiguously conclude in favor of component reconnection we need to measure the magnetic shear at the X-line in more cases, possibly in a more accurate way than done in Paper I.

- How do magnetic field and plasma decouple in the diffusion region? Which micro-processes do ultimately trigger the explosive large-scale behavior of reconnection? To answer this question, we need more observations of reconnection close to the X-line. However, this is difficult to achieve just because spacecraft crossings are rare there. Nevertheless, observations done in the separatrix regions extending from the X-line can overcome this limitation and provide important information about the microphysics in the diffusion region.

- What is the relationship between the diffusion region and the separatrix region? Is the diffusion region localized around the X-point or it extends along the separatrix regions far away? Numerical simulations and other observations indicate that the latter could be the case e.g. parallel electric

fields exist all the way along the separatrices and not only around the X-line. More observations of the diffusion region and of the separatrix region are necessary in the future to address this point.

From a more general point of view other issues about reconnection and transport mechanisms in general should also be considered in future:

- How mass, momentum and energy can be transferred across boundary layers in collisionless space plasmas?
- What is the relative importance of other proposed mechanisms compared to magnetic reconnection?
- What is the best definition of magnetic reconnection?
- What is the importance of magnetic reconnection in other systems than the Earth's magnetosphere, for example in astrophysical plasmas?

In this thesis we have used observations of reconnection at the magnetopause only. However, there is another region in the Earth's magnetosphere that plays a key role for magnetic reconnection: the magnetotail. It would be interesting in the future to investigate these issues using magnetotail observations also. In the magnetotail the scales are different compared to those at the magnetopause and also reconnection is not directly driven by the solar wind but we expect to observe the same basic physical processes there.

Acknowledgements

First I want to thank my supervisor Prof. Mats André for giving me the privilege to work within the Cluster project at the Swedish Institute of Space Physics. He has supported my scientific work in many ways. Through him, I want to acknowledge the Swedish National Space Board for the essential financial support.

I am very much grateful to my assistant supervisor Dr. Andris Vaivads for his constant and patient every-day support, not only on the scientific side. I have learned much from him and I am glad that I can work with him still for a while.

I acknowledge the personnel at IRF-U, scientific and not, for their collaboration. In particular Dr. Yuri Khotyaintsev and Dr. Michiko Morooka for their help with Cluster data.

Also, I want to thank all the PhD students at IRF-U. Some of the 'doktorander' have become in these years also good friends. I am grateful to Rico Behlke for providing the template and for other practical suggestions about how to make this thesis.

Last but not least on the professional side, I want to thank all the Cluster community members for their efforts to make this mission working in the good way as it does now. In particular, fruitful collaboration with Dr. M. Bice Bavassano Cattaneo and Dr. M. Federica Marcucci at IFSI, Roma is acknowledged.

Then it's time for friends and family. I will be brief, for important things one doesn't need many words. I want to thank all my friends, the 'old' ones and the 'new' ones. Among the new ones here in Uppsala, Luca Giacomelli, for sharing with me in these last years good and bad moments. Last, my family, 'old' and 'new' members: Adele, Anna, Anja, Anselmo, Paolo, Pippo, Sascha and Selma. Thanks for your confidence in me. Without you all my every-day efforts to do a good job make no sense.

Bibliography

[1] http://sci.esa.int/science-e-media/img/32/Image3-410.jpg.

[2] http://sci.esa.int/science-e-media/img/83/ClusterSeasonalOrbits.jpg.

[3] http://sci.esa.int/science-e-media/img/f6/31318.jpg.

[4] W. I. Axford. Viscous interaction between the solar wind and the Earth's magnetosphere. *Plan. Space Sci.*, 12:45–+, January 1964.

[5] W. Baumjohann and R.A. Treumann. *Basic space plasma physics*. Imperial College Press, London, 1996.

[6] S. W. H. Cowley. Magnetic reconnection. In E. R. Priest, editor, *Solar system magnetic fields*. D. Reidel Publ. Co., Dordrecht, The Netherlands, 1986.

[7] S. W. H. Cowley. Theoretical Perspectives of the Magnetopause: A Tutorial Review. In *Physics of the Magnetopause*. American Geophysical Union, 1995.

[8] T.E. Cravens. *Physics of solar system plasmas*. Cambridge University Press, Cambridge, 1997.

[9] N. U. Crooker. Dayside merging and cusp geometry. *J. Geophys. Res.*, 84(13):951–959, March 1979.

[10] P.W. Daly. *Users Guide to the Cluster Science Data System*. European Space Agency, 2002.

[11] C. Day. Spacecraft probes the site of magnetic reconnection in earth's magnetotail. *Physics Today*, 54:16–17, October 2001.

[12] F. de Hoffmann and E. Teller. Magneto-Hydrodynamic Shocks. *Physical Review*, 80:692–703, November 1950.

[13] J. W. Dungey. Interplanetary Magnetic Field and the Auroral Zones. *Phys. Rev. Lett.*, 6:47–48, January 1961.

[14] C. P. Escoubet, M. Fehringer, and M. Goldstein. The Cluster mission. *Ann. Geophys.*, 19:1197–1200, 2001.

[15] S. A. Fuselier, K. J. Trattner, and S. M. Petrinec. Cusp observations of high- and low-latitude reconnection for northward interplanetary magnetic field. *J. Geophys. Res.*, 105(14):253–266, January 2000.

[16] R. G. Giovanelli. A theory of chromospheric flares. *Nature*, 158:81–82, 1946.

[17] H. Hasegawa, M. Fujimoto, T.-D. Phan, H. Rème, A. Balogh, M. W. Dunlop, C. Hashimoto, and R. Tandokoro. Transport of solar wind into Earth's magnetosphere through rolled-up Kelvin-Helmholtz vortices. *Nature*, 430:755–758, August 2004.

[18] M. Hesse and K. Schindler. A theoretical foundation of general magnetic reconnection. *J. Geophys. Res.*, 93(12):5559–5567, June 1988.

[19] L. C. Lee. A Review of Magnetic Reconnection: MHD Models. In *Physics of the Magnetopause*. American Geophysical Union, 1995.

[20] R. H. Levy. Aerodynamic aspects of the magnetospheric flow. *AIAA J.*, 12:2065–2076, 1964.

[21] A. T. Y. Lui, C. Jacquey, G. S. Lakhina, R. Lundin, T. Nagai, T.-D. Phan, Z. Y. Pu, M. Roth, Y. Song, R. A. Treumann, M. Yamauchi, and L. M. Zelenyi. Critical Issues on Magnetic Reconnection in Space Plasmas. *Space Sci. Rev.*, 116:497–521, January 2005.

[22] R. Lundin, J.-A. Sauvaud, H. Rème, A. Balogh, I. Dandouras, J. M. Bosqued, C. Carlson, G. K. Parks, E. Möbius, L. M. Kistler, B. Klecker, E. Amata, V. Formisano, M. Dunlop, L. Eliasson, A. Korth, B. Lavraud, and M. McCarthy. Evidence for impulsive solar wind plasma penetration through the dayside magnetopause. *Ann. Geophy.*, 21:457–472, February 2003.

[23] F. S. Mozer, S. D. Bale, and T. D. Phan. Evidence of Diffusion Regions at a Subsolar Magnetopause Crossing. *Phys. Rev. Lett.*, 89(1):015002–+, June 2002.

[24] F. S. Mozer, S. D. Bale, T. D. Phan, and J. A. Osborne. Observations of Electron Diffusion Regions at the Subsolar Magnetopause. *Phys. Rev. Lett.*, 91(24):245002–+, December 2003.

[25] E. N. Parker. Sweet's Mechanism for Merging Magnetic Fields in Conducting Fluids. *J. Geophys. Res.*, 62(11):509–520, 1957.

[26] G. Paschmann, I. Papamastorakis, N. Sckopke, G. Haerendel, B. U. O. Sonnerup, S. J. Bame, J. R. Asbridge, J. T. Gosling, C. T. Russel, and R. C. Elphic. Plasma acceleration at the earth's magnetopause - Evidence for reconnection. *Nature*, 282:243–246, November 1979.

[27] H. E. Petschek. Magnetic Field Annihilation. In *The Physics of Solar Flares*, pages 425–+, 1964.

[28] T. Phan, H. U. Frey, S. Frey, L. Peticolas, S. Fuselier, C. Carlson, H. Rème, J.-M. Bosqued, A. Balogh, M. Dunlop, L. Kistler, C. Mouikis, I. Dandouras, J.-A. Sauvaud, S. Mende, J. McFadden, G. Parks, E. Moebius, B. Klecker, G. Paschmann, M. Fujimoto, S. Petrinec, M. F. Marcucci, A. Korth, and R. Lundin. Simultaneous Cluster and IMAGE observations of cusp reconnection and auroral proton spot for northward IMF. *Geophy. Res. Lett.*, 30:16–1, May 2003.

[29] E. Priest and T. Forbes. *Magnetic reconnection.* Cambridge University Press, Cambridge, 2000.

[30] B. Rossi and S. Olbert. *Introduction to the physics of space.* McGraw-Hill, New York, 1970.

[31] C. T. Russell and R. C. Elphic. Initial ISEE magnetometer results - Magnetopause observations. *Space Sci. Rev.*, 22:681–715, December 1978.

[32] K. Schindler, M. Hesse, and J. Birn. General magnetic reconnection, parallel electric fields, and helicity. *J. Geophys. Res.*, 93(12):5547–5557, June 1988.

[33] D. G. Sibeck, G. Paschmann, R. A. Treumann, S. A. Fuselier, W. Lennartsson, M. Lockwood, R. Lundin, K. W. Ogilvie, T. G. Onsager, T.-D. Phan, M. Roth, M. Scholer, N. Sckopke, K. Stasiewicz, and M. Yamauchi. Chapter 5-Plasma Transfer Processes at the Magnetopause. *Space Sci. Rev.*, 88:207–283, 1999.

[34] B. U. O. Sonnerup, I. Papamastorakis, G. Paschmann, and H. Luehr. Magnetopause properties from AMPTE/IRM observations of the convection electric field - Method development. *J. Geophy. Res.*, 92(11):12137–12159, November 1987.

[35] B. U. O. Sonnerup, I. Papamastorakis, G. Paschmann, and H. Luehr. The magnetopause for large magnetic shear - Analysis of convection electric fields from AMPTE/IRM. *J. Geophy. Res.*, 95(14):10541–10557, July 1990.

[36] B. U. O. Sonnerup, G. Paschmann, I. Papamastorakis, N. Sckopke, G. Haerendel, S. J. Bame, J. R. Asbridge, J. T. Gosling, and C. T. Russell. Evidence for magnetic field reconnection at the earth's magnetopause. *J. Geophys. Res.*, 86(15):10049–10067, November 1981.

[37] P. A. Sweet. The Neutral Point Theory of Solar Flares. In *Electromagnetic Phenomena in Cosmical Physics*, Proceedings from IAU Symposium no. 6. Cambridge University Press, 1958.

[38] R. A. Treumann and W. Baumjohann. *Advanced space plasma physics.* Imperial College Press.

[39] A. Vaivads, Y. Khotyaintsev, M. André, A. Retinò, S. C. Buchert, B. N. Rogers, P. Décréau, G. Paschmann, and T. D. Phan. Structure of the Magnetic Reconnection Diffusion Region from Four-Spacecraft Observations. *Phys. Rev. Lett.*, 93(10):105001–+, August 2004.

[40] M. Yamauchi, R. Lundin, O. Norberg, I. Sandahl, L. Eliasson, and D. Winningham. Signature of direct magnetosheath plasma injections onto closed field-line regions based on observations at mid- and low-altitudes. In P. Newell and T. Onsager, editors, *Earth's Low-Latitude Boundary Layer - Geophysical Monograph Series 133* . American Geophysical Union, 2003.

Paper I

A. Retinò, M. B. Bavassano Cattaneo, M. F. Marcucci, A. Vaivads, M. André, Y. Khotyaintsev, T. Phan, G. Pallocchia, H. Rème, E. Möbius, B. Klecker, C.W. Carlson, M. McCarthy, A. Korth, R. Lundin, and A. Balogh.

Cluster multispacecraft observations at the high-latitude dusk side magnetopause: implications for continuous and component magnetic reconnection.

Annales Geophysicae , 23, 461 – 473, 2005.

Annales Geophysicae (2005) 23: 461–473
SRef-ID: 1432-0576/ag/2005-23-461

Annales Geophysicae

Cluster multispacecraft observations at the high-latitude duskside magnetopause: implications for continuous and component magnetic reconnection

A. Retinò[1], M. B. Bavassano Cattaneo[2], M. F. Marcucci[2], A. Vaivads[1], M. André[1], Y. Khotyaintsev[1], T. Phan[3], G. Pallocchia[2], H. Rème[4], E. Möbius[5], B. Klecker[6], C. W. Carlson[3], M. McCarthy[7], A. Korth[8], R. Lundin[9], and A. Balogh[10]

[1]Swedish Institute of Space Physics, Uppsala, Sweden
[2]IFSI-CNR, Roma, Italy
[3]University of California, Berkeley, USA
[4]CESR, Toulouse, France
[5]University of New Hampshire, Durham, USA
[6]MPE, Garching, Germany
[7]University of Washington, Seattle, USA
[8]MPS, Lindau, Germany
[9]Swedish Institute of Space Physics, Kiruna, Sweden
[10]Imperial College, London, UK

Received: 28 May 2004 – Revised: 15 October 2004 – Accepted: 21 October 2004 – Published: 28 February 2005

Abstract. We report multispacecraft Cluster observations of magnetic reconnection at the high-latitude magnetopause/magnetospheric boundary layer (MP/BL) under mainly northward interplanetary magnetic field (IMF) conditions. The event we study is on 3 December 2001 when the Cluster spacecraft were skimming the high-latitude duskside MP/BL during a period of about four hours. The orbit and configuration of the spacecraft were such that at least one satellite was present in the MP/BL during most of that period. We present the evidence of reconnection in the form of tangential stress balance between the magnetosheath and the MP/BL (Walén test) and in several cases in the form of transmitted magnetosheath ions in the MP/BL and incident/reflected magnetosheath ions in the magnetosheath boundary layer (MSBL) . The observations are consistent with magnetic reconnection occurring tailward of the cusp and going on continuously for a period of about four hours. The observed directions of the reconnection flows are consistent with the IMF orientation, thus indicating that reconnection is globally controlled by the IMF. Observations of a few flow reversals suggest passages of the spacecraft close to the X-line. The observation of low magnetic shear across the magnetopause during a flow reversal is consistent with component merging at least in one case. The observation of reconnection flows on the duskside magnetopause irrespective of the change in the sign of the IMF B_Y also suggests a better agreement with the component merging model, though antiparallel merging cannot be excluded because the distance from the X-line is not known.

Key words. Magnetospheric physics (magnetopause, cusp and boundary layers; solar wind-magnetosphere interactions) – Space plasma physics (magnetic reconnection)

Correspondence to: A. Retinò
(alessandro.retino@irfu.se)

1 Introduction

Magnetic reconnection on the Earth's magnetopause is considered to be the most efficient mechanism to transfer mass, momentum and energy from the solar wind to the Earth's magnetosphere (Cowley, 1984). Evidence of magnetic reconnection can be fluid and/or kinetic. The fluid (MHD) evidence is the tangential stress balance across the magnetopause/magnetospheric boundary layer (MP/BL), the so-called Walén test (Hudson, 1970; Paschmann et al., 1979, 1986; Sonnerup et al., 1981). The kinetic evidence is in the form of observations of particle distribution functions on reconnected field lines, such as transmitted magnetosheath ions in the MP/BL and reflected magnetosheath ions in the magnetosheath boundary layer (MSBL)(Cowley, 1982, 1995; Fuselier, 1995). The fluid and kinetic evidence gives complementary information about the occurrence of reconnection and are mutually consistent (Gosling et al., 1990; Bauer et al., 2001; Phan et al., 2001).

At high-latitudes reconnection occurs tailward of the cusp for northward IMF. Evidence of high-latitude reconnection consists of accelerated sunward ion flows in the lobes and of D-shaped distribution functions for the ions transmitted across the magnetopause, as established by in-situ observations (Gosling et al., 1991, 1996; Kessel et al., 1996; Safrankova et al., 1998; Avanov et al., 2001; Phan et al., 2003). In this study we find similar evidence of magnetic reconnection on the duskside high-latitude magnetopause tailward of the cusp under mainly northward IMF.

Important questions related to the large-scale nature of the reconnection are its continuity in time and the location of the X-line on the magnetopause. The reconnection process is considered continuous if it continues for extended time without interruption, as opposed to intermittent reconnection. Continuity implies that the reconnection rate never drops to zero even though it can be variable. The variability in time of the reconnection rate determines whether the process is steady or unsteady. When the rate is almost constant in time, the reconnection is considered quasi-steady. At low latitudes for southward IMF in-situ evidence of long lasting reconnection flows on a time scale of few hours has been interpreted in terms of quasi-steady reconnection (Gosling et al., 1982; Phan et al., 2000; Marcucci et al., 2000). At high-latitude indications of continuous reconnection active for several hours have been obtained directly from in-situ observations by Phan et al. (2004) for southward IMF. Indirect evidence of continuous reconnection has been obtained from proton aurora measurements by Frey et al. (2003) with northward IMF and from radar measurements by Pinnock et al. (2003) with southward IMF. The possibility to infer the continuity of the reconnection process at the magnetopause from in-situ measurements is limited. The in-situ evidence, such as plasma jets or ion distribution functions on reconnected field lines, can be observed only during a short time interval when a spacecraft crosses the MP/BL. No information on the reconnection can be obtained when a spacecraft is well inside/outside the magnetosphere even if the process is actually going on continuously. Nevertheless, the possibility to have many simultaneous observations points as with Cluster reduces this limitation (Phan et al., 2004), especially for particularly favorable orbit and spacecraft configurations. As a result of such conditions in our study, we are able to obtain observations that are consistent with magnetic reconnection going on continuously for a period of about four hours.

Another important issue is the location of the X-line, a place where the reconnection is initiated. According to large-scale models of reconnection, the location of the X-line is controlled by the relative orientation of the IMF and the Earth's magnetic field. Different models predict different locations of the X-line. In the antiparallel merging model (Crooker, 1979; Luhmann et al., 1984) the reconnection occurs in localized regions at the magnetopause where the magnetic fields are nearly antiparallel. On the other hand, in the component merging model (Sonnerup, 1974; Gonzalez and Mozer, 1974) the reconnection can occur even if only one component of the magnetosheath and magnetospheric magnetic field is oppositely directed. In general, it is difficult to conclude whether the component or the antiparallel merging model best describes the large-scale configuration of magnetic reconnection at the high-latitude magnetopause without knowing the location of the X-line, which has been inferred in a quantitative way using measurements in the Earth's magnetospheric cusp (Fuselier et al., 2000) and in a qualitative way using proton aurora measurements (Fuselier et al., 2002; Phan et al., 2003). On the basis of cusp aurora observations, Fuselier et al. (2002) concluded that under northward IMF high-latitude reconnection can be better explained by antiparallel merging. In this description the location of the X-line is limited to a localized region on the magnetopause and it depends on the value of the IMF B_Y component i.e. the X-line moves to the dawn/dusk flank of the magnetopause for any finite dusk/dawn IMF B_Y component. Nevertheless, recent observations show that at high-latitude with northward IMF antiparallel and component reconnection can occur at the same time (Trattner et al., 2004). In this interpretation reconnection occurs at the high-latitude magnetopause also where it is not predicted by the antiparallel merging model, the only difference being that the process is less efficient than in the antiparallel situation.

A good way to distinguish between the two models is to measure the magnetic shear in the vicinity of the X-line. This is in general difficult because passages close to the X-line are rare. Nevertheless, in some fortuitous cases passages close to the reconnection site can be detected when ion jet reversals are observed (Avanov et al., 2001; Phan et al., 2003). In these cases a measurement of the local magnetic shear gives an indication of the shear at the X-line. Here we report two examples of X-line encounters detected using the observations of ion jet reversals. One of them has low magnetic shear which is inconsistent with antiparallel merging predictions.

In our study we present multispacecraft Cluster observations of high-latitude magnetic reconnection tailward of the cusp under northward IMF conditions. We find fluid and kinetic evidence of reconnection and we conclude that reconnection can be continuous for several hours and that the location of the X-line on the high-latitude magnetopause can be better explained by the component merging model.

The paper is structured in the following way. In Sect. 2 we describe the data set and the orbit/configuration of Cluster during the event. In Sect. 3 we describe the observations of the overall event while in Sect. 4 we concentrate on the selection and analysis of the accelerated flows. Section 5 describes the fluid and kinetic reconnection tests on the accelerated flows. Finally, in Sect. 6 we discuss the results and summarize them in Sect. 7.

2 Data set and orbit

In this study we present observations during the time interval 07:35–11:55 UT on 3 December 2001. We use data from the Cluster Ion Spectrometry (CIS) and the Flux-Gate Magnetometer (FGM) experiments on board Cluster

spacecraft SC/1, SC/3 and SC/4. No data from CIS are available for SC/2. The CIS experiment consists of two different instruments: CODIF, which provides the three-dimensional ion distribution function of four ions species (H^+, He^+, He^{++} and O^+) in the energy per charge range 20–40 000 eV/e, and HIA which gives the ion three-dimensional distribution function in the energy per charge range 5–32 000 eV/e with no mass separation (Reme et al., 2001). Both instruments have a time resolution up to the spacecraft spin period (4 s). Distribution functions and onboard moments with 4 s time resolution are used in this study. Data from CIS-HIA for ions are used for SC/1 and SC/3 while data from CIS-CODIF for H^+ are used for SC/4. The FGM experiment is described by Balogh et al. (2001). Spin-averaged magnetic field data with 4 s time resolution are used for all the spacecraft. Solar wind parameters have been obtained from the ACE spacecraft.

Figure 1 shows the Cluster orbit in the GSM YZ and XZ planes during the event. The spacecraft are located in the duskside Southern Hemisphere and move, during the event, from $-65°$ to $-50°$ in GSM latitude and from 17:00 to 15:00 in GSM local time. The separation between the spacecraft during this event is several thousand kilometers in the GSM YZ plane (see the insert in Fig. 1) and is smaller along the X_{GSM} direction (not shown), namely 500 km between SC1 and SC/3, and 1200 km between SC/4 and SC/3, with SC/3 always at the largest X_{GSM}.

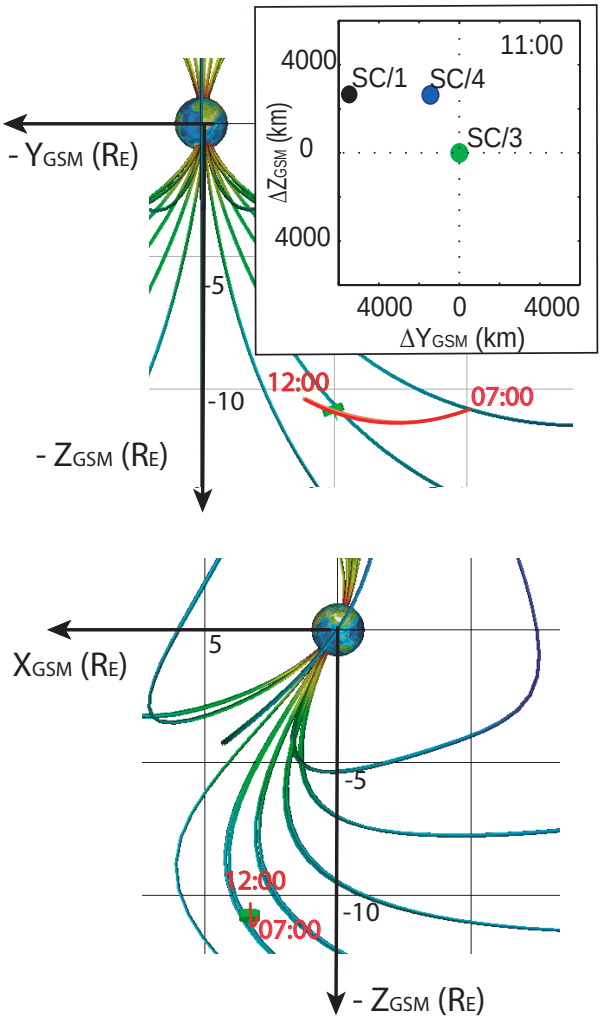

Fig. 1. SC/3 orbit on GSM XY and YZ planes from 07:00 UT to 12:00 UT on 3 December 2001. The spacecraft position corresponds to 11:00 UT. The insert shows SC/1 and SC/4 location respect to SC/3 on GSM YZ plane at 11:00 UT. The plot was created using the OVT program (http://ovt.irfu.se).

3 Observations

3.1 Event overview

Figure 2 is a summary plot of the event in the interval 07:35–11:55 UT. The four top panels show the ion energy spectrogram, the ion number density, the velocity components and magnetic field components in GSE for SC/1. The following panels show the same quantities for SC/3 and SC/4, respectively. Until 08:50 UT SC/4 was operating in the low sensitivity mode (it uses the hemisphere of the detector with the small geometrical factor). At the beginning of the interval all three spacecraft are in the magnetosheath. SC/1 and SC/4 have an inbound magnetopause crossing at approximately the same time, around 07:40 UT. After that time, during the whole event, they stay mainly on the magnetospheric side of the MP performing crossings of the current sheet mostly before 09:00 UT. Simultaneously with the SC/1 and SC/4 MP crossing at 07:40 UT, SC/3 goes from the magnetosheath into a turbulent sheath-like region close to the current sheet, as indicated by many partial crossings, staying there until 09:40 UT when the spacecraft has a complete MP crossing. This crossing is followed by several other crossings until the end of the event. As shown by the data, SC/3 spends more time than the other two spacecraft in the magnetosheath (from 07:40 to 09:40 UT and during several time intervals between 09:40 and 11:55 UT).

Two points are noteworthy. First, the orientation of the magnetospheric magnetic field ($B_X<0$, $B_Y>0$, $B_Z<0$) indicates that the spacecraft are located on the dusk side of the magnetopause tailward of the cusp. Secondly, due to the particular configuration of the spacecraft with respect to the magnetopause, at least one spacecraft is close to the magnetopause throughout the event. This shows a clear advantage of having multiple observation points in studies of reconnection as the number of current sheet encounters increases.

The main feature of this event is that during most of the magnetopause crossings, both complete and partial, the spacecraft observe “anomalous” flows in the MP/BL, namely flows which differ from the usual MP/BL flow, being either sunward flows in the opposite direction to the magnetosheath flow or antisunward jets with a speed larger than the magnetosheath speed. These flows are interpreted as being due to magnetic reconnection and are the subject of the present study. They will be discussed in Sects. 4 and 5 but first we describe the solar wind conditions.

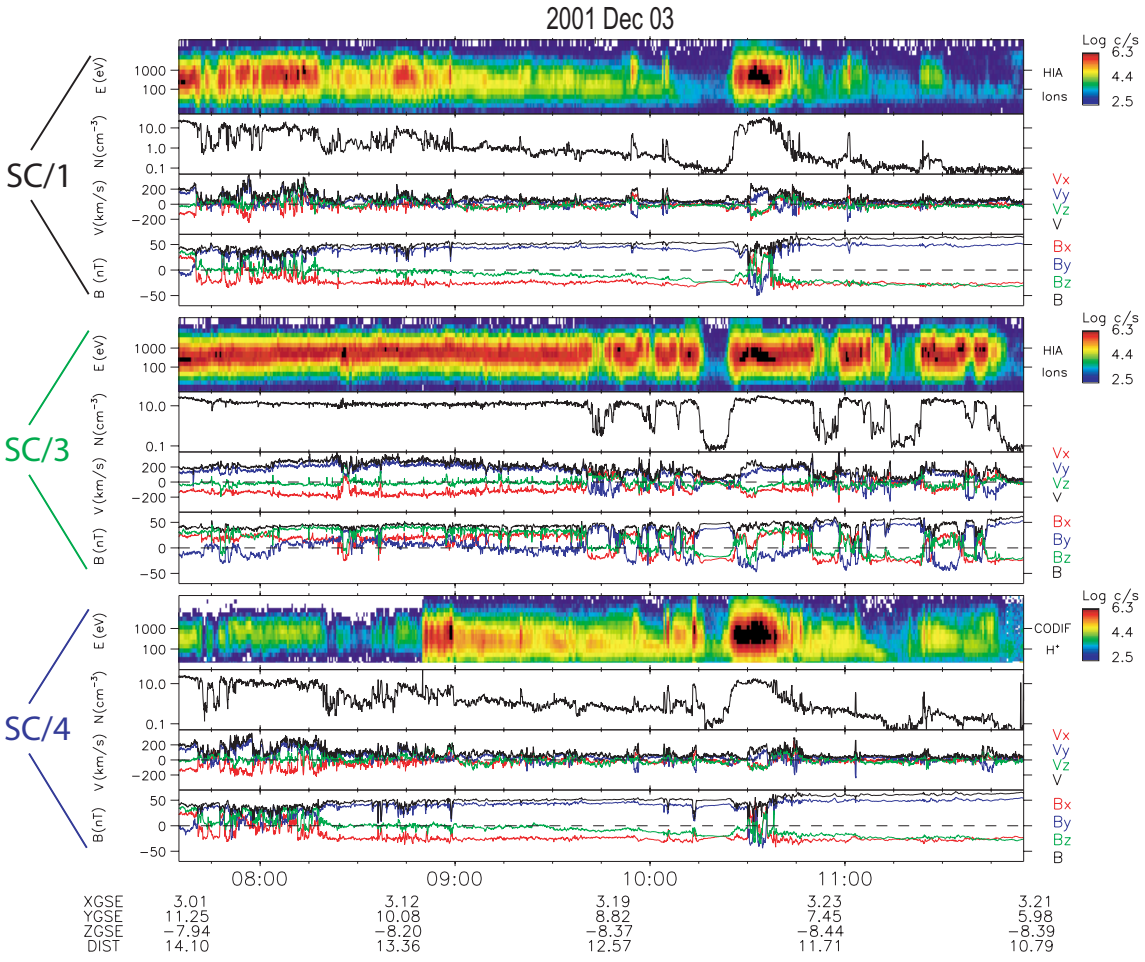

Fig. 2. Summary plot of the event from 07:35 to 11:55 UT . The four top panels show ion energy spectrogram, ion number density, ion velocity components and magnetic field components in GSE for SC/1. The following panels show the same quantities for SC/3 and SC/4, respectively.

3.2 Solar wind conditions

In this event we are in the ideal situation of having a nearby solar wind monitor directly in the magnetosheath: this is SC/3, which spends most of the time in the magnetosheath. The comparison between the magnetic field on SC/3 and on ACE has shown that, when SC/3 is in the magnetosheath, it sees similar features as ACE, although with variable delays. The IMF B_Z is the dominant component and it stays mainly positive during the event (except for brief negative excursions). The IMF B_Y is more variable, it is mainly positive or zero in the first part of the event (from 07:35 to 09:40 UT) and mainly negative in the second part (from 09:40 to 11:55 UT, except for an interval of positive values from 10:40 to 10:50 UT). For this reason the MP crossings have low magnetic shear in the earlier part of the event (i.e. before 09:40 UT) and high magnetic shear later.

Another important feature of the solar wind conditions is that the magnetosheath flow adjacent to the MP is sub-Alfvénic during most of the event. The Alfvénic Mach number M_A, calculated from SC/3 velocity (in the intervals when the spacecraft was in the magnetosheath) is quite low, typically about 0.5, as one can see in Fig. 3, for a short time interval.

4 Examples of anomalous flows

Figure 3 is an example of two complete magnetopause crossings, one inbound and one outbound, observed by SC/3 over a short time interval. At both crossings anomalous flows are present in the MP/BL. From 10:47:00 to 10:49:49 UT SC/3 is in the magnetosheath (except for a brief excursion in the MP between 10:48:45 and 10:49:37 UT). From 10:49:49 to 10:50:25 UT it performs a complete inbound crossing of the current sheet, as shown by the density and temperature gradient and by the magnetic field rotation. From 10:49:51 to 10:50:15 UT and from 10:50:27 to 10:50:39 UT SC/3 observes, respectively, an accelerated antisunward flow ($V_X<0$, $V_Y>0$, $V_Z<0$) greater than adjacent magnetosheath values and a sunward flow ($V_X>0$, $V_Y<0$, $V_Z>0$). Later, from 10:58:14 to 10:58:38 UT it crosses the current sheet for the

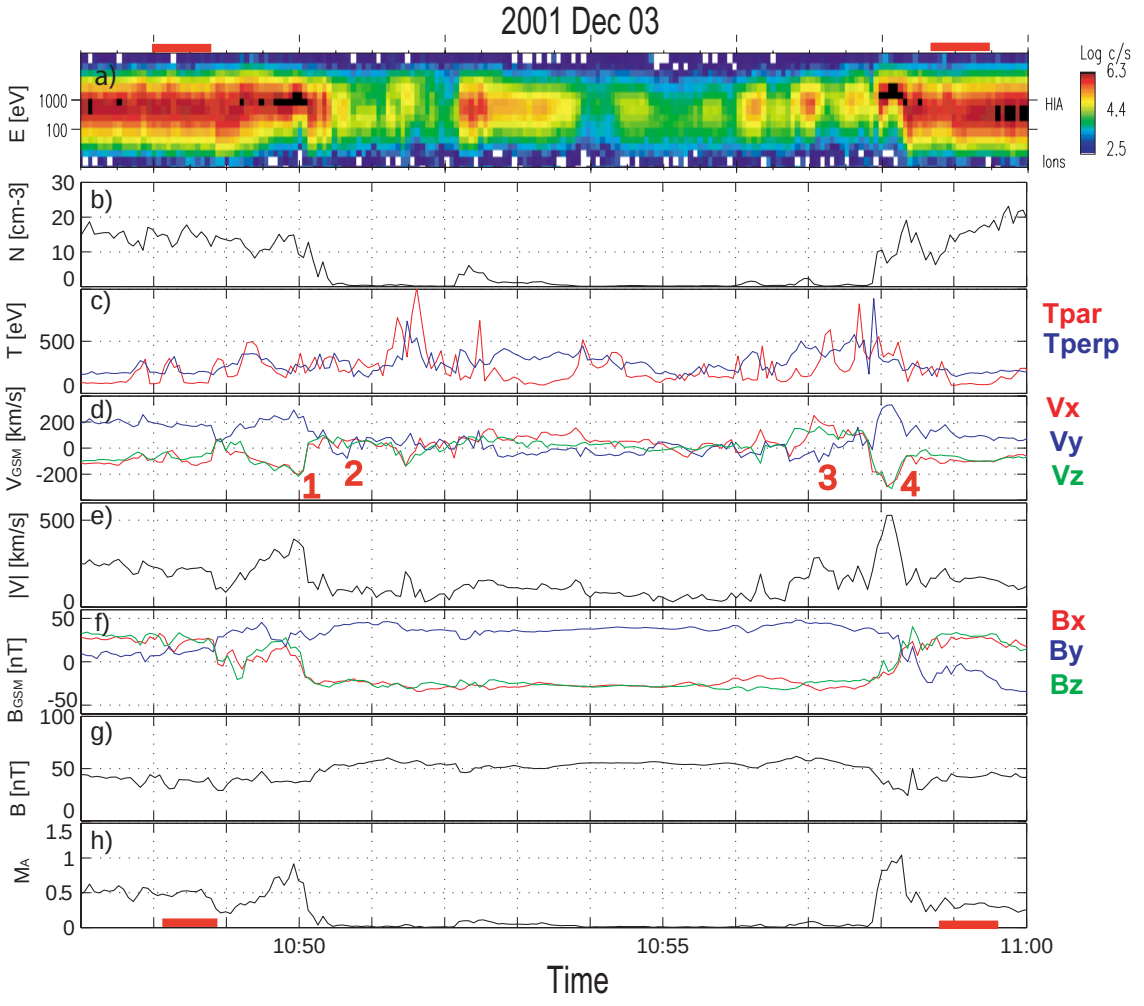

Fig. 3. Ion and magnetic field data for SC/3 in the time interval 10:47–11:00 UT. Panels show from top to bottom: **(a)** ion energy spectrogram, **(b)** ion number density, **(c)** parallel and perpendicular ion temperatures, **(d)** ion velocity components in GSM, **(e)** ion total velocity, **(f)** magnetic field components in GSM, **(g)** total magnetic field and **(h)** Alfvénic Mach number. Reconnection flows are indicated by red labels 1–4 while magnetosheath reference levels are shown by horizontal red bars.

second time, as shown again by the density and temperature gradient and by the magnetic field rotation. From 10:56:44 to 10:57:16 UT and from 10:57:52 to 10:58:16 UT SC/3 observes, respectively, a sunward flow ($V_X>0$, $V_Y<0$, $V_Z>0$) and an accelerated antisunward flow ($V_X<0$, $V_Y>0$, $V_Z<0$). Finally, after 10:58:38 SC/3 is in the magnetosheath.

The data described in Fig. 3 show examples of anomalous flows occurring in the MP/BL during complete magnetopause crossings (total rotation of magnetic field). Other anomalous flows occur during partial magnetopause crossings (partial or no rotation of magnetic field), usually when the spacecraft goes from the magnetosphere to the MP/BL without entering the magnetosheath proper.

Sunward directed flows ($V_X>0$) are mainly observed in the BL while tailward flows ($V_X<0$) are observed mainly in the MP. Both types of accelerated flows are the object of the present study and we interpret them in terms of high-latitude magnetopause reconnection. Such interpretation of sunward flows, directed in the opposite direction to the expected mantle/lobe velocity, has been done previously for other events (Gosling et al., 1991, 1996; Kessel et al., 1996; Safrankova et al., 1998; Avanov et al., 2001; Popescu et al., 2001; Phan et al., 2003).

5 Evidence of magnetic reconnection

In this section we discuss the fluid and kinetic evidence of magnetic reconnection. The fluid analysis is discussed in more detail while only qualitative considerations are given about the kinetic analysis. Also, the mutual consistency of both is briefly discussed.

5.1 Fluid evidence of reconnection

In order to test reconnection, the Walén test (Hudson, 1970; Paschmann et al., 1979, 1986; Sonnerup et al., 1981) was

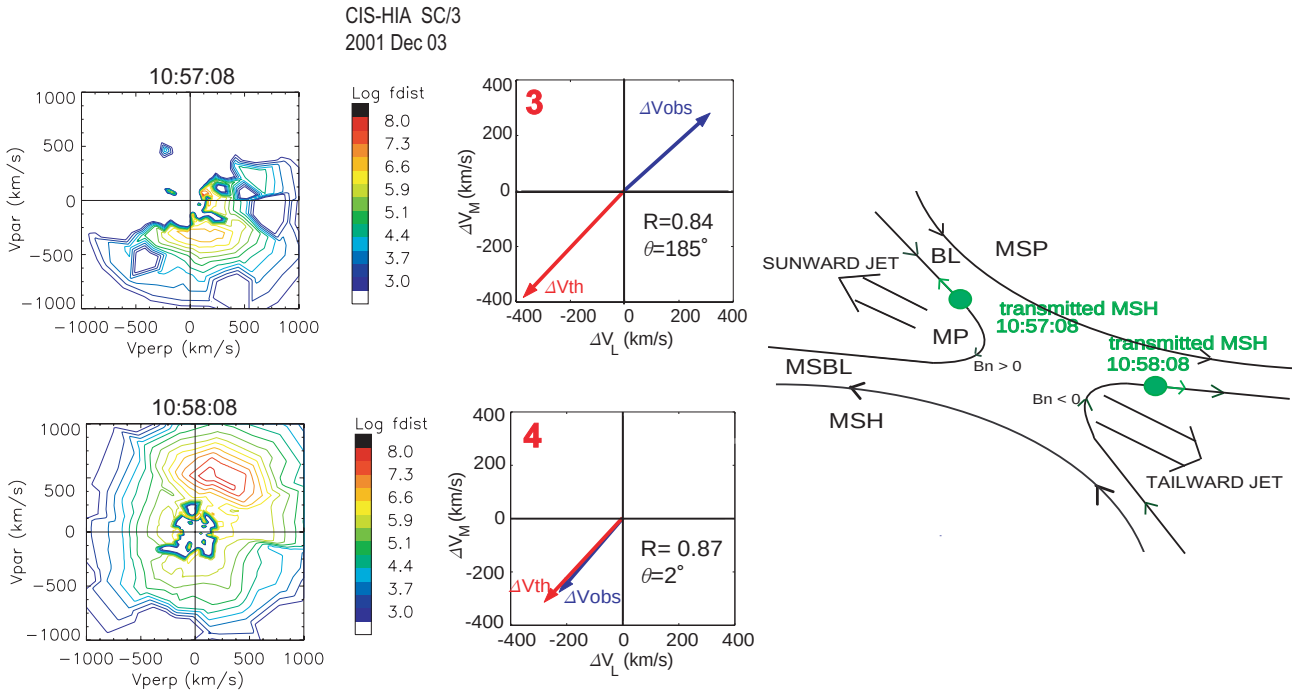

Fig. 4. D-shaped distribution functions on the $(V_\perp, V_\parallel)$ plane and Walén test on the (L,M) plane for the flow reversal observed by SC/3 between 10:57:08 and 10:58:08 UT. R is the ratio $|\Delta \boldsymbol{V}_{obs}|/|\Delta \boldsymbol{V}_{th}|$ while θ is the angle between the two vectors $\Delta \boldsymbol{V}_{obs}$ and $\Delta \boldsymbol{V}_{th}$ on the (L,M) plane. A perfect agreement would result in antisymmetric vectors for the sunward jet (R=1, θ=180°) and overlapping vectors for the tailward jet (R=1, θ=0°). The reconnection geometry is sketched on the right.

performed. In this test the tangential stress balance for a rotational discontinuity is achieved comparing the two vectors $\Delta \boldsymbol{V}_{t,obs}=\boldsymbol{V}_{2t}-\boldsymbol{V}_{1t}$ and

$$\Delta \boldsymbol{V}_{t,th} = \pm[(1-\alpha_1)\mu_0\rho_1]^{1/2} \cdot [\boldsymbol{B}_{2t}(1-\alpha_2) - \boldsymbol{B}_{1t}(1-\alpha_1)] \quad (1)$$

where $\boldsymbol{V}$ is the bulk velocity, ρ the density, $\boldsymbol{B}$ the magnetic field and $\alpha=(p_\parallel-p_\perp)\mu_0/B^2$ the pressure anisotropy factor. The subscript t indicates the component of a vector in the plane tangent to the magnetopause while the subscripts *th*, *obs* indicates theoretical and observed values, respectively. The two vectors are evaluated in the local (L,M) plane tangent to the magnetopause (Russell and Elphic, 1978) and calculated in a magnetosheath reference point (subscript 1) and in a point in the MP/BL (subscript 2).

As an example of Walén test, we perform the Walén analysis for the interval 10:47:00–11:00 UT, shown in Fig. 3. This interval includes a complete inbound crossing around 10:50 UT and a complete outbound crossing around 10:58 UT. Two local reference intervals (indicated in Fig. 3 by horizontal red bars) are used, the first from 10:48:23 to 10:48:47 UT, and the second from 10:58:48 to 10:59:37 UT. With the first reference level we have tested the two jets at 10:50:03 UT (antisunward) and 10:50:36 UT (sunward) labelled, respectively, 1 and 2 in Fig. 3 while with the second reference level we have tested the two jets at 10:57:08 UT (sunward) and 10:58:08 UT (antisunward) labelled 3 and 4 in the same figure. The result of the Walén test shows an excellent agreement with the theoretical predictions for reconnection at all four jets, as reported in Fig. 4, central panels, for jets 3 and 4, where $\Delta \boldsymbol{V}_{t,obs}$ and $\Delta \boldsymbol{V}_{t,th}$ are drawn in the local (L,M) plane. The ratio $R=|\Delta \boldsymbol{V}_{t,obs}|/|\Delta \boldsymbol{V}_{t,th}|$ and the angle θ between the two vectors is also reported for the two jets 3 and 4. The other panels of Fig. 4 will be discussed in Sect. 5.2.

The Walén test has been performed across all the complete MP crossings using a local reference level. It was decided to exclude from the Walén test the interval in which SC/4 was operating in low sensitivity mode (namely before 08:50 UT), although also in this interval SC/4 detects anomalous flows. In low sensitivity mode two polar sectors are absent; this has only a limited impact on moment calculation in the magnetosheath and magnetosphere but could strongly affect the moments in the case of anomalous flows.

SC/1 and SC/4 detect anomalous flows not only during the complete MP crossings, but also during occasional passes into the BL from the magnetosphere. These passes occur mainly between 8:30–10:15 UT, and are identified by a density gradient. The magnetic field rotation is partial or absent. The Walén analysis can be performed also on these partial crossings because SC/3 continuously provides a reference level in the magnetosheath. So even in the absence of a substantial rotation of the magnetic field, the Walén test can be performed across the MP between a point in the BL observed by SC/1 or SC/4 and a point in the magnetosheath, simultaneously observed by SC/3. This procedure assumes that over the separation of the spacecraft (few thousands kilometers)

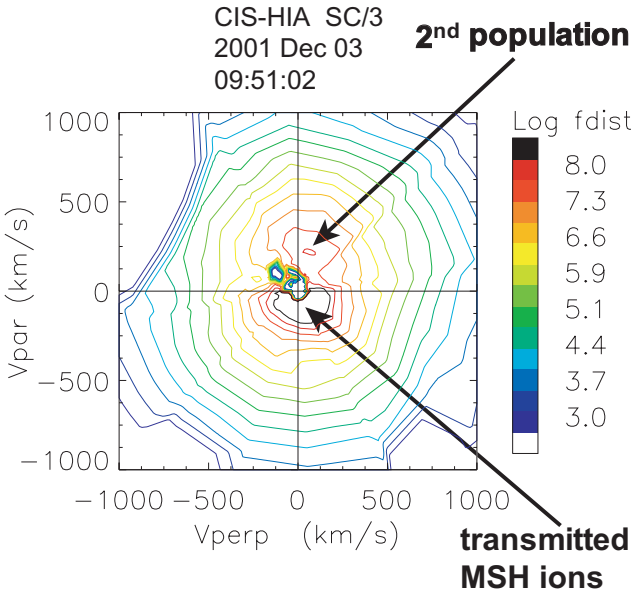

Fig. 5. SC/3 ion distribution function on the $(V_\perp, V_\parallel)$ plane at 09:51:02 UT when the spacecraft is in the current sheet. A second population parallel to the magnetic field is present besides the transmitted magnetosheath ions.

the conditions in the magnetosheath are mainly unchanged.

When testing reconnection on all the complete and partial MP encounters, it was found that, while the Walén test is generally well satisfied in the outer part of the BL which is close to the MP (i.e. close to the field rotation), it usually becomes worse both in the MP and in the inner part of the BL close to the magnetosphere proper. The poor result of the Walén test in the inner BL/magnetosphere is qualitatively in agreement with previous analysis (Phan et al., 2001). A possible explanation of the worsening of the test in the MP is that quite often, besides the expected transmitted magnetosheath ions, additional populations (which are being investigated in detail in an ongoing study) are observed inside the MP. As an example, HIA observations during an MP crossing of SC/3 at 09:51:02 UT are shown in Fig. 5. Two populations are present: one antiparallel to the magnetic field, which we interpret to be the transmitted magnetosheath population, and a second population. The Walén test considerably improves if the moments of the distribution function are computed after removing the second population. This has been verified in a few, but representative, examples, as shown in Table 1. The improvement of the Walén test after the removal of the second population is consistent with the interpretation in terms of magnetic reconnection because the effect of the additional population is to modify the bulk velocity used in the Walén test (Gosling et al., 1996).

The results of the Walén analysis for the whole event are reported in Fig. 6c as a function of time. This figure is meant to illustrate in a synthetic way the results of the analysis for this long lasting event with numerous MP crossings observed by the three spacecraft. At each complete or partial

Table 1. Result of Walén test before and after the removal of the second population for some reconnection jets observed by SC/3.

	$\lvert\Delta V_{obs}\rvert/\lvert\Delta V_{th}\rvert$		θ	
Time	before	after	before	after
09:51:02	0.73	0.86	221	170
09:57:51	0.18	0.58	194	180
09:58:39	0.40	0.62	177	170
11:36:51	0.28	0.76	156	174
11:37:51	0.38	0.65	152	180

magnetopause crossing, the ratio R and the angle θ defined above have been evaluated between a reference level in the magnetosheath (subscript 1 in Eq. 1) and each data point of an anomalous flow inside the MP/BL (subscript 2 in Eq. 1). In order to ensure that we are considering plasma of magnetosheath origin, a density criterion was applied, and only BL intervals with $n>1\,\mathrm{cm}^{-3}$ were considered. To assure an acceptable degree of confidence on the analysis results we consider the Walén test to be satisfied if the magnitude of the ratio R differs by less than 0.3 from unity and the angle differs by less than 20° from its theoretical value (0° or 180°). For each interval of anomalous flow satisfying the Walén relation, only the point with the best value of R and θ has been retained and reported in Fig. 6c. In this figure each point is represented by a segment with magnitude equal to R and inclination equal to the same angle as that between ΔV_{obs} and ΔV_{th} on the (L,M) plane. Notice that several such segments can correspond to one MP crossing. Complete (partial) MP crossings are indicated by full (dashed) lines. A perfect Walén test with a plus (minus) sign, namely with an inward (outward) B_n component, would give a vertical segment of unit length, pointing up (down) for antisunward (sunward) flows. The horizontal black lines indicate intervals in which all three spacecraft are far from the current sheet (either in the magnetosheath, or in the magnetosphere). Note that panels (a) and (b) of Fig. 6 will be described in Sect. 6.3.

Figure 6c shows that reconnection flows are observed throughout the event by the three spacecraft. Indeed, out of 27 complete magnetopause crossings observed by the three spacecraft, 22 show accelerated flows which satisfy the Walén relation. Of the remaining five crossings, three are outbound magnetopause crossings experienced by the three spacecraft around 10:25 UT, possibly associated to a brief southward turning of the IMF when reconnection is not expected to occur tailward of the cusp. Moreover, one crossing of the BL (SC/3 at 09:59 UT) is possibly too fast to be able to detect jets, and the other (SC/3 at 11:05:38 UT) is slightly below our selection criteria (R=0.66, θ=159°).

Most of the observed jets flow sunward, consistent with the reconnection site being tailward of the spacecraft. Few antisunward flows are also observed, indicating that the reconnection site was sometimes sunward of the spacecraft. Tailward flows are detected mainly by SC/3, consistent with

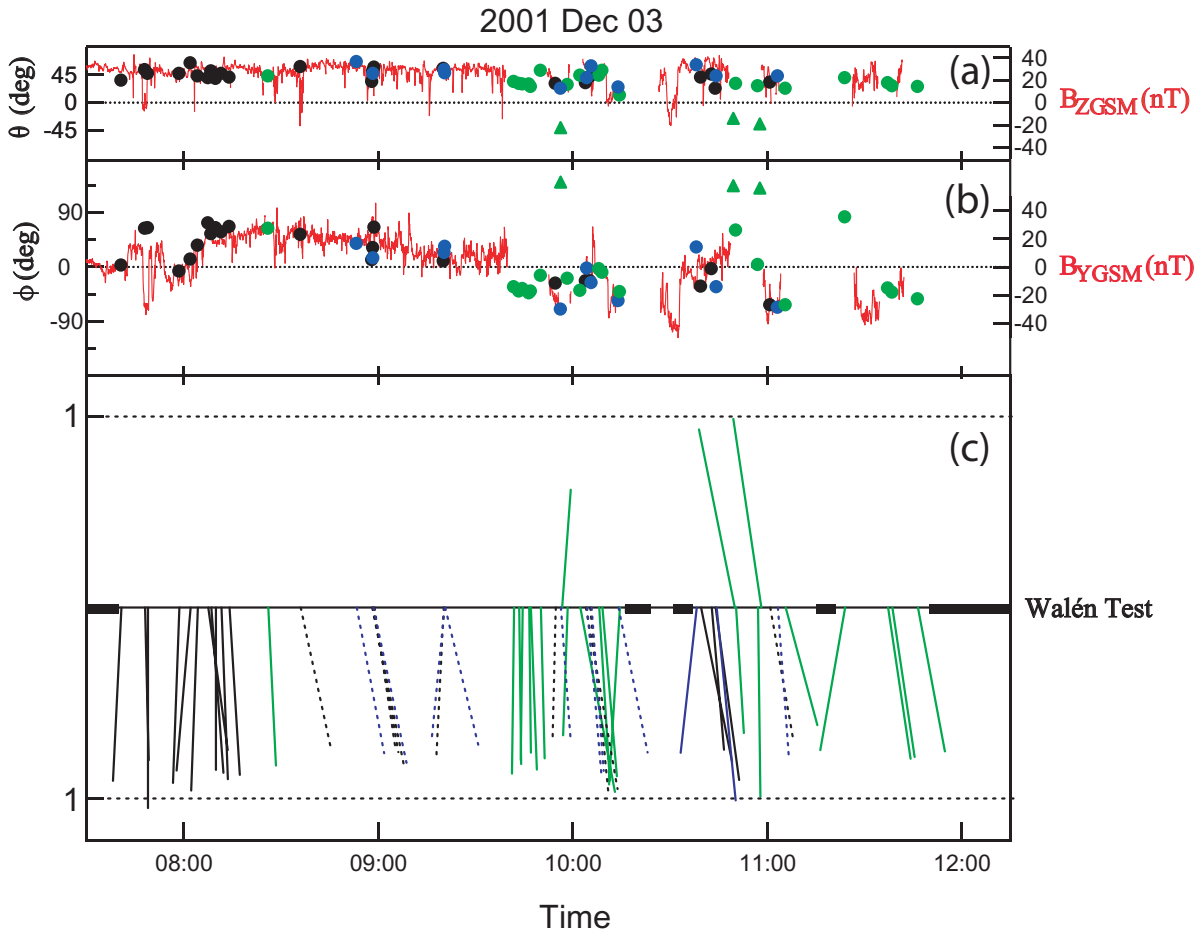

Fig. 6. Walén test and direction of the reconnection jets. **(a)** Superposed latitude θ_{GSM} and SC/3 $B_{Z\,GSM}$, **(b)** superposed longitude ϕ_{GSM} and SC/3 $B_{Y\,GSM}$, **(c)** temporal history of the Walén test during the event. Sunward flows are indicated by circles while antisunward flows by triangles. SC/1 data are in black, SC/3 data in green, SC/4 data in blue. Reconnection jets associated with complete/partial crossings are indicated by full/dashed lines. A perfect Walén test would give a vertical vector of unit length, pointing up (down) for antisunward (sunward) flows. Horizontal black bars indicate intervals when all the SCs are far from the MP/BL.

its position being more tailward with respect to the other spacecraft and therefore being more favorable to detect tailward flows.

5.2 Kinetic evidence of reconnection

Several kinetic signatures typical of reconnection (Cowley, 1995) have often been observed during this event: (1) D-shaped distribution function of transmitted magnetosheath ions in the MP/BL; (2) incident/reflected magnetosheath ions in the magnetosheath boundary layer (MSBL). D-shaped distribution functions are expected in the MP/BL with a low-energy cutoff at a velocity $V_{\parallel}$ along the magnetic field equal to the parallel component of the deHoffmann-Teller velocity (Cowley, 1982). These distributions functions, although not present at all reconnection flow events on this day, have been observed in many cases. For example, in the partial MP crossing around 09:55 by SC/1 and SC/4, all the distribution functions (during about 1 min) are D-shaped. Two examples are shown in Fig. 4 for SC/3 at 10:57:08 and 10:58:08 UT. The distributions show a low energy cut-off at a velocity parallel to the magnetic field with $V_{\parallel}<0$ at 10:57:08 UT (sunward flow i.e. $B_n>0$) and $V_{\parallel}>0$ at 10:58:08 UT (tailward flow i.e. $B_n<0$). In this figure a sketch of the reconnection geometry is also shown. An explicit calculation of the deHoffman-Teller reference frame for the tailward flow shows good agreement with theoretical expectations of $V_{\parallel}-V_{HT\parallel}\approx 280$ km/s and $V_{cut\parallel}\approx 250$ km/s, where $V_{cut\parallel}$ is the observed cut-off along the magnetic field in the distribution function at 10:58:08 UT.

We also observe incident/reflected magnetosheath ions in the MSBL in some cases. The reflected magnetosheath ions are expected to flow in the MSBL along the magnetic field lines in the opposite direction to the incident population. One example is shown in Fig. 7 for SC/3. Incident and reflected populations have the expected velocities $V_{i\parallel}<0$ and $V_{r\parallel}>0$ for a MSBL adjacent to a sunward jet ($B_n>0$), as shown in the sketch of the reconnection geometry.

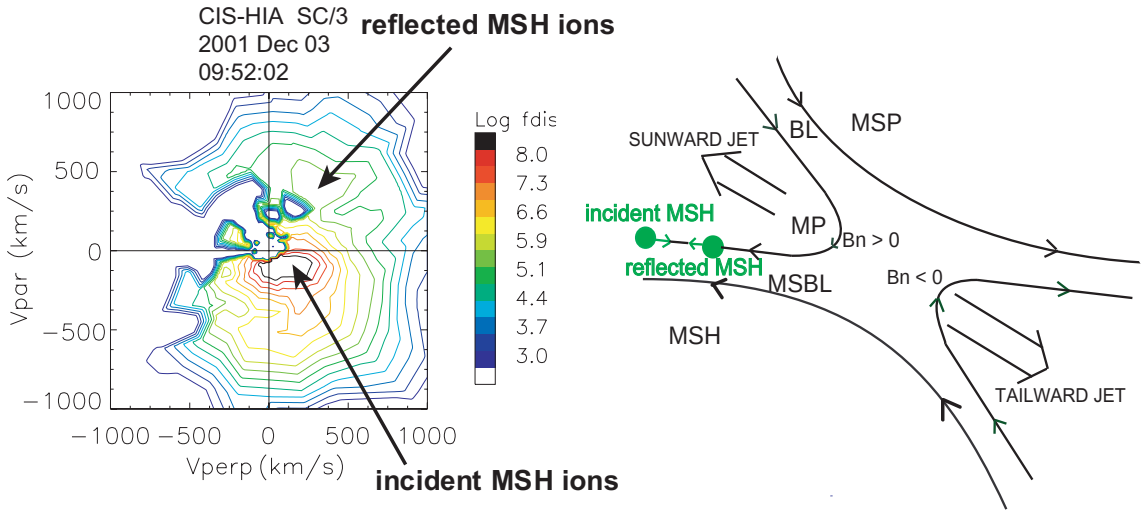

Fig. 7. SC/3 ion distribution function on the $(V_\perp, V_\parallel)$ plane at 09:52:22 UT when the spacecraft is in the MSBL. Incident and reflected populations are shown, as well as a sketch of the reconnection geometry.

5.3 Consistency between fluid and kinetic evidence

Fluid and kinetic signatures of magnetic reconnection are both observed during this event but with larger occurrence for fluid evidence, in agreement with previous studies (Bauer et al., 2001). In a few cases both evidence is observed at the same time showing mutual consistency: (a) for sunward flows: Walén relation satisfied with negative sign (implying $B_n>0$, i.e. crossing sunward of the reconnection site), D-shaped distribution functions in the MP/BL, with cut-off at $V_\parallel<0$, and incident/reflected MSBL populations with $V_{i\parallel}<0$ and $V_{r\parallel}>0$; (b) for tailward flows: Walén relation satisfied with positive sign (implying $B_n<0$, i.e. crossing tailward of the reconnection site), D-shaped distribution functions in the MP/BL with cut-off at $V_\parallel>0$.

6 Discussion

6.1 Evidence of magnetic reconnection

During about four hours the Cluster spacecraft, separated by a distance of a few thousands kilometers, observe anomalous flows, i.e. either sunward flows in the direction opposite to the magnetosheath flow or antisunward jets with a speed larger than the magnetosheath speed. These flows are in agreement with the occurrence of magnetic reconnection, as shown by the satisfactory result of the Walén test (fluid evidence). Kinetic signatures, in the form of D-shaped distribution functions for transmitted magnetosheath ions in the MP/BL and of incident/reflected magnetosheath ions in the MSBL, also confirm this interpretation in some cases. Fluid evidence is observed more often than kinetic evidence. When the two pieces of evidence are found together, they show mutual consistency.

Additional ion populations, other than the expected transmitted magnetosheath ions, are often present in the MP and in those cases the Walén test gives poor agreement, but after their removal from the distribution function the Walén test shows a general improvement. This is consistent with theoretical expectations, if additional ion populations do not cross the magnetopause (Gosling et al., 1996). The detailed study of these additional populations is the subject of an ongoing study.

Finally, it is important to notice that sunward flows can be observed during this event because of a quite low Alfvénic Mach number ($\approx$0.5) in the magnetosheath throughout the event. This condition is expected to hold for observation of sunward convection in the lobes as result of high-latitude reconnection tailward of the cusp (Gosling et al., 1991; Popescu et al., 2001).

6.2 Continuity of the reconnection process

The orbit and the configuration of the spacecraft during this event are just ideal to address the continuity issue. The spacecraft are skimming the MP in such a way that for most of the time SC/3 is close to the MP on the magnetosheath side while SC/1 and SC/4 are in the BL. The separation between the spacecraft is of the order of the magnetopause thickness, i.e. about one thousand kilometers, so that normally at least one spacecraft is inside the magnetopause. Only during a few time intervals were all three spacecraft well inside the magnetosphere or well outside in the magnetosheath. As a result of this convenient combination of spacecraft configuration and orbit, the number of MP/BL encounters increased, resulting in an excellent coverage of the magnetopause.

We argue that our observations are consistent with continuous reconnection occurring at the high-latitude magnetopause during about four hours. Figure 6c shows that reconnection flows are repeatedly detected throughout the time of observations. They are observed at all complete MP crossings (except at five crossings discussed earlier) and, thanks

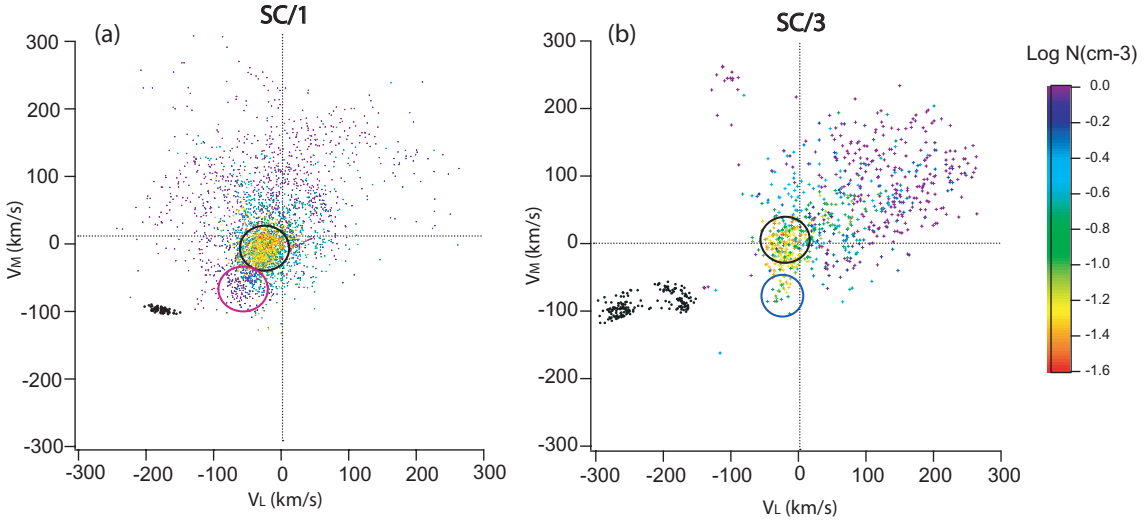

Fig. 8. Scatter plot of SC/1 (left) and SC/3 (right) ion flow velocity for all the magnetosphere and boundary layer passages. Color coding corresponds to the logarithm of the ion number density. The black dots are representative of magnetosheath flow. See the text for the description of circles.

to Cluster's configuration, also at many partial crossings of SC/1 and SC/4 so that, all together, a large number of reconnection flows are detected during four hours. This strongly suggests that reconnection can be continuous. Of course, one cannot exclude the possibility that the reconnection process ceases between the jets, which usually corresponds to time intervals when the spacecraft are far from the MP/BL (black horizontal bars in Fig. 6c). If reconnection is continuous, reconnection flows should be present every time the spacecraft are in the MP/BL. This condition cannot be tested quantitatively for all the anomalous flows observed in the MP/BL, first because they correspond to too many data points, and second because it is difficult to exclude data points in the inner BL/magnetosphere, where the Walén test is not expected to work. Nevertheless, in Fig. 8 we show a qualitative indication that most of the time the spacecraft are in the BL they observe anomalous sunward directed flows while they do not observe them in the magnetosphere proper. Figure 8 shows a scatter plot of (V_L,V_M) ion flow velocity for all the magnetosphere and BL passes. The magnetosphere proper has been schematically identified as the region of dipole magnetic field with ion density smaller than 1 cm^{-3}, while the BL is identified as the region of dipole-like magnetic field with ion density greater than 1 cm^{-3}. The data points are color coded according to the corresponding density. The left panel refers to SC/1 and the right panel to SC/3. The black dots in the lower left quadrant of each plot are representative of magnetosheath flow. Points inside black circles and inside the blue circle are flows in the magnetosphere and in the mantle. It is found that apart from a few points, indicated by a red circle in panel (a), SC/1 and SC/3 observe sunward anomalous flows whenever they are in the BL, but not in the magnetosphere proper, where the velocity has the typical features of the mantle/lobe velocity.

It is important to stress that the Walén test gives no information about the reconnection rate. As long as continuous reconnection jets are observed, one can only conclude that the reconnection process is continuous in time (i.e. the reconnection rate is different from zero). However, this does not imply a steady reconnection because the reconnection rate can still be modulated in time (Phan et al., 2004).

6.3 IMF control of reconnection on large scale

Mainly sunward flows are observed during the event, implying that an X-line is located tailward of the spacecraft most of the time. Because spacecraft are located tailward of the cusp this is consistent with the X-line being tailward of the cusp, in agreement with mainly northward IMF conditions. A few tailward flows are observed by SC/3 sometimes indicating an X-line sunward of the spacecraft.

Figure 6 shows the flow directions of each reconnection event in terms of latitude θ_{GSM} (panel a) and longitude ϕ_{GSM} (panel b), defined on the XY_{GSM} plane to be zero for Y_{GSM}=0 and positive in the anticlockwise direction. The IMF B_Z and B_Y components (measured by SC/3 in the magnetosheath) are also shown, superposed, respectively, on θ_{GSM} and on ϕ_{GSM}. The antisunward flows are observed with $\theta_{GSM}<0°$ and $\phi_{GSM}>90°$. The sunward flows are instead observed with $\theta_{GSM}>0°$ and ϕ_{GSM} from positive/zero (before 09:40 UT) to negative (after 09:40 UT), with an absolute value less than 90°. The sign of ϕ_{GSM} seems to follow the change in the sign of the IMF B_Y, from positive during the first part of the event to negative during the second part. Therefore, the pattern of the flow directions during the whole event is consistent with the orientation of the reconnecting IMF. This indicates that the reconnection process is globally controlled by the IMF rather than being a local random process (Nishida, 1989).

6.4 Component vs. antiparallel merging

It is possible to qualitatively distinguish between antiparallel and component merging when spacecraft are close to the X-line because the relevant parameter is the magnetic shear at the X-line. Ion jet reversals have been interpreted as a possible indication of the spacecraft passage close to the X-line (Gosling et al., 1991; Avanov et al., 2001; Phan et al., 2003). Figure 3 shows two jet reversals observed by SC/3 on a time interval of about 10 min. The first one, around 10:50 UT, shows a passage from a tailward jet (indicated by the label 1 in the figure) to a sunward jet (label 2) while the second, around 10:58 UT, shows a passage from a sunward jet (label 3) to a tailward jet (label 4). All four observed flows are consistent with the occurrence of magnetic reconnection and both fluid and kinetic evidence (D-shaped distribution functions) have been found. Thus, we interpret these two jet reversals as passages of SC/3 close to the X-line.

As one can see from the figure the first MP crossing at 10:50 UT has low shear (100°), being $B_Y>0$ while the second one has high shear (160°), being $B_Y<0$ instead. Taking the jet reversals as indications of passages close to the reconnection site one can regard the measured shear to be close to the shear at the X-line. For crossings 1 and 2 the observations seem to be more consistent with component merging because of the small shear measured close to the reconnection site. The fact that the velocities (both tailward and sunward) observed during crossings 1 and 2 are smaller than those observed during crossings 3 and 4 is also consistent with component merging because of the weaker "kick" experienced by the injected ions compared to the antiparallel situation (Trattner et al., 2004). A sketch of component merging for this event is given in Fig. 9, where the reconnection geometry on the duskside is shown. Observations of sunward flows with $\theta_{GSM}>0°$ and $\phi_{GSM}>0°$ are consistent with component merging, for which freshly opened field lines cannot give enough "kick" to the ions to flow in the $\phi_{GSM}<0°$. The observations of reconnection flows far out on the dusk side of the magnetopause, irrespective of the change in the IMF B_Y, also support component merging as discussed below.

In the second part of the event (after 09:40 UT), while IMF B_Y stays mainly negative, jets are recorded in the sunward-dawnward ($\phi_{GSM}<0°$) and northward ($\theta_{GSM}>0°$) direction, except in three cases when tailward jets are recorded by SC/3. This is consistent with reconnection site located almost always tailward and southward of the spacecraft during this interval. The local shear measured by the spacecraft in this part of the event is close to the antiparallel prediction, apart from the time interval 10:40–10:50 UT, during which IMF B_Y is positive. In this situation it is not possible to distinguish between the antiparallel and component merging models, which both predict an X-line in the Southern Hemisphere on the dusk flank where the spacecraft are located.

In the first part of the event (before 09:40 UT) jets are directed northward ($\theta_{GSM}>0°$) but now $\phi_{GSM}\geq 0°$, i.e. jets are directed sunward and duskward. This is consistent again with a reconnection site located tailward and southward of the spacecraft. During this interval the IMF B_Y is mainly positive. For this orientation of the IMF the antiparallel merging predicts an X-line on the dawn side of the magnetopause in the Southern Hemisphere, i.e. on the opposite side of where the spacecraft are located. Cluster is located at $Y_{GSM}=5-10\ R_E$ which is far from the possible antiparallel reconnection site. According to component merging reconnection could still occur on the dusk side of the magnetopause, close to the Cluster location. The local shear measured by the spacecraft in this part of the event is far from the antiparallel prediction. Nevertheless this evidence cannot be used to conclusively rule out antiparallel merging, except for the case of flow reversals, because the X-line could be far away from the spacecraft and no information about the distance from the X-line is available.

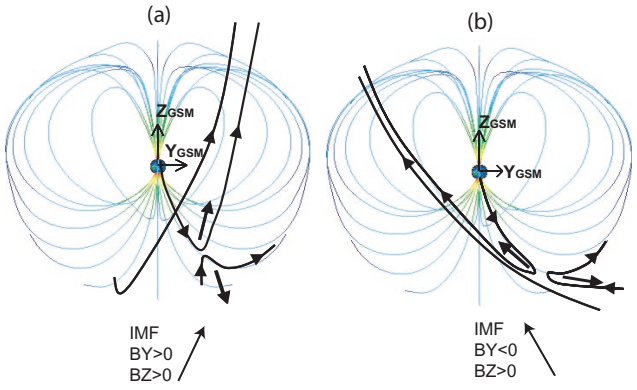

Fig. 9. Reconnection configuration for the two orientations of IMF. **(a)** IMF $B_Z>0$, $B_Y>0$, **(b)** IMF $B_Z>0$, $B_Y<0$. The jet directions are represented by the arrows.

7 Summary and conclusions

In this paper we analyze, in detail, Cluster observations at the high-latitude duskside magnetopause on 3 December 2001. We show fluid and kinetic evidence of magnetic reconnection which strongly suggests that reconnection is continuous for a period of about four hours:

1. The fluid evidence is substantiated by the good agreement of the observed accelerated flows with the tangential stress balance between the magnetosheath and the magnetopause/magnetospheric boundary layer (Walén test). The kinetic evidence consists of the observation of D-shaped ion distribution functions in some reconnection flows in the magnetopause/magnetospheric boundary layer and of observations of incident/reflected magnetosheath ions in the magnetosheath boundary layer. When found together, fluid and kinetic evidence are consistent with each other.

2. Inside the magnetopause, besides the expected transmitted magnetosheath ions, the ion distribution functions often show additional populations. The Walén test

improves after their removal from the distribution function, as shown in a few cases.

3. Observations are consistent with magnetic reconnection going on continuously for about four hours whenever the IMF is northward. Most of the time when no reconnection flows are observed the spacecraft are far from the magnetopause. The extended time coverage was possible due to the particularly favorable orbit and configuration of the spacecraft during this event. Out of a total number of 27 all but 5 complete magnetopause crossings are associated with reconnection flows. The other observed reconnection flows are associated with partial magnetopause crossings.

The observations are consistent with large-scale IMF control of magnetic reconnection and suggest a better agreement with component merging model:

1. During the event the IMF is mainly northward and the observations are consistent with magnetic reconnection occurring tailward of the cusp, as expected. Mainly sunward flows are observed during the event, implying that an X-line is located tailward of the spacecraft most of the time.

2. Flow directions during the event are consistent with the orientation of the reconnecting IMF. Observations are not consistent with patchy reconnection.

3. Observations of a few ion flow reversals indicate passages of the spacecraft close to the X-line.

4. During one of the flow reversals we observe low magnetic shear across the magnetopause on the side of the magnetosphere where an X-line is not predicted by antiparallel merging model. The observed low shear is consistent with a component merging model. The observations of reconnection flows far out on the dusk side of the magnetopause, irrespective of a change in the sign of the IMF B_Y, also suggest component merging model but they cannot be used to conclusively exclude antiparallel merging because the X-line could be far away from the spacecraft.

Acknowledgements. We thank the ACE/MAG team for interplanetary magnetic field data. The work done at IFSI has been supported by the Agenzia Spaziale Italiana. A. Retinò is supported by the Swedish National Space Board.

Topical Editor T. Pulkkinen thanks R. L. Kessel and another referee for their help in evaluating this paper.

References

Avanov, L. A., Smirnov, V. N., Waite, J. H., Fuselier, S. A., and Vaisberg, O. L.: High-latitude magnetic reconnection in sub-Alfvénic flow: Interball tail observations on May 29, 1996, J. Geophys. Res., 29 491–29 502, 2001.

Balogh, A., Carr, C. M., Acuña, M. H., Dunlop, M. W., Beek, T. J., Brown, P., Fornacon, K. H., Georgescu, E., Glassmeier, K. H., Harris, J., Musmann, G., Oddy, T., and Schwingenschuh, K.: The Cluster Magnetic Field Investigation: overview of in-flight performance and initial results , Ann. Geophys., 19, 1207–1217, 2001,
SRef-ID: 1432-0576/ag/2001-19-1207.

Bauer, T. M., Paschmann, G., Sckopke, N., Treumann, R. A., Baumjohann, W., and Phan, T. D.: Fluid and particle signatures of dayside reconnection, Ann. Geophys., 19, 1045–1063, 2001,
SRef-ID: 1432-0576/ag/2001-19-1045.

Cowley, S. W. H.: The causes of convection in the Earth's magnetosphere – A review of developments during the IMS, Rev. Geophys. Space Phys., 20, 531–565, 1982.

Cowley, S. W. H.: Evidence for the occurrence and importance of reconnection between the Earths magnetic field and the interplanetary magnetic field, in: AGU Geophysical Monograph 30, edited by: Hones, E. W., 375–378, American Geophysical Union, 1984.

Cowley, S. W. H.: Theoretical perspectives of the magnetopasue: a Tutorial Review, in: AGU Geophysical Monograph 90, edited by: Song, P., Sonnerup, B., and Thomsen, M., 29–43, American Geophysical Union, 1995.

Crooker, N. U.: Dayside merging and cusp geometry, J. Geophys. Res., 84, 951–959, 1979.

Frey, H. U., Phan, T. D., Fuselier, S. A., and Mende, S. B.: Continuous magnetic reconnection at Earth's magnetopause, Nature, 426, 533–537, 2003.

Fuselier, S. A.: Kinetic Aspects of reconnection at the Magnetopause, in: AGU Geophysical Monograph 90, edited by: Song, P., Sonnerup, B., and Thomsen, M., 181–187, American Geophysical Union, 1995.

Fuselier, S. A., Petrinec, S. M., and Trattner, K. J.: Stability of the high-Latitude reconnection site for steady northward IMF, Geophys. Res. Lett., 27, 473, 2000.

Fuselier, S. A., Frey, H. U., Trattner, K. J., Mende, S. B., and Burch, J. L.: Cusp aurora dependence on interplanetary magnetic field B_z, J. Geophys. Res., 107, 6–1, 2002.

Gonzalez, W. D. and Mozer, F. S.: A quantitative model for the potential resulting from reconnection with an arbitrary interplanetary magnetic field, J. Geophys Res., 79, 4186–4194, 1974.

Gosling, J. T., Asbridge, J. R., Bame, S. J., Feldman, W. C., Paschmann, G., Sckopke, N., and Russell, C. T.: Evidence for quasi-stationary reconnection at the dayside magnetopause, J. Geophys. Res., 87, 2147–2158, 1982.

Gosling, J. T., Thomsen, M. F., Bame, S. J., Onsager, T. G., and Russell, C. T.: The electron edge of the low latitude boundary layer during accelerated flow events, Geophys. Res. Lett., 17, 1833–1836, 1990.

Gosling, J. T., Thomsen, M. F., Bame, S. J., Elphic, R. C., and Russell, C. T.: Observations of reconnection of interplanetary and lobe magnetic field lines at the high-latitude magnetopause, J. Geophys. Res., 96, 14 097–14 106, 1991.

Gosling, J. T., Thomsen, M. F., Le, G., and Russell, C. T.: Observations of magnetic reconnection at the lobe magnetopause, J. Geophys. Res., 101, 24 765–24 774, 1996.

Hudson, P. D.: Discontinuities in an anisotropic plasma and their identification in the solar wind, Planet. Space Sci., 18, 1611–1622, 1970.

Kessel, R. L., Chen, S.-H., Green, J. L., Fung, S. F., Boardsen, S. A., Tan, L. C., Eastman, T. E., Craven, J. D., and Frank, L. A.: Evidence of high-latitude reconnection during northward IMF:

Hawkeye observations, Geophys. Res. Lett., 23, 583, 1996.

Luhmann, J. G., Walker, R. J., Russell, C. T., Crooker, N. U., Spreiter, J. R., and Stahara, S. S.: Patterns of potential magnetic field merging sites on the dayside magnetopause, J. Geophys. Res., 89, 1741–1744, 1984.

Marcucci, M. F., Bavassano Cattaneo, M. B., di Lellis, A. M., Cerulli Irelli, P., Kistler, L. M., Phan, T.-D., Haerendel, G., Klecker, B., Paschmann, G., Baumjohann, W., Möbius, E., Popecki, M. A., Sauvaud, J. A., Rème, H., Korth, A., et al.: Evidence for interplanetary magnetic field B_y controlled large-scale reconnection at the dayside magnetopause, J. Geophys. Res., 27 497–27 508, 2000.

Nishida, A.: Can random reconnection on the magnetopause produce the low latitude boundary layer?, Geophys. Res. Lett., 16, 227–230, 1989.

Paschmann, G., Papamastorakis, I., Sckopke, N., Haerendel, G., Sonnerup, B. U. O., Bame, S. J., Asbridge, J. R., Gosling, J. T., Russel, C. T., and Elphic, R. C.: Plasma acceleration at the Earth's magnetopause – Evidence for reconnection, Nature, 282, 243–246, 1979.

Paschmann, G., Baumjohann, W., Sckopke, N., Papamastorakis, I., and Carlson, C. W.: The magnetopause for large magnetic shear – AMPTE/IRM observations, J. Geophys. Res., 91, 11 099–11 115, 1986.

Phan, T. D., Kistler, L. M., Klecker, B., Haerendel, G., Paschmann, G., Sonnerup, B. U. Ö., Baumjohann, W., Bavassano-Cattaneo, M. B., Carlson, C. W., DiLellis, A. M., Fornacon, K.-H., Frank, L. A., Fujimoto, M., Georgescu, E., Kokubun, S., Moebius, E., Mukai, T., Øieroset, M., Paterson, W. R., and Reme, H.: Extended magnetic reconnection at the Earth's magnetopause from detection of bi-directional jets, Nature, 404, 848–850, 2000.

Phan, T. D., Sonnerup, B. U. Ö., and Lin, R. P.: Fluid and kinetics signatures of reconnection at the dawn tail magnetopause: Wind observations, J. Geophys. Res., 106, 25 489–25 502, 2001.

Phan, T. D., Frey, H. U., Frey, S., Peticolas, L., Fuselier, S., Carlson, C., Rème, H., Bosqued, J.-M., Balogh, A., Dunlop, M., Kistler, L., Mouikis, C., Dandouras, I., Sauvaud, J.-A., Mende, S., McFadden, J., Parks, G., Moebius, E., Klecker, B., Paschmann, G., Fujimoto, M., Petrinec, S., Marcucci, M. F., Korth, A., and Lundin, R.: Simultaneous Cluster and IMAGE observations of cusp reconnection and auroral proton spot for northward IMF, Geophys. Res. Lett., 30, 16–1, 2003.

Phan, T. D., Dunlop, M. W., Paschmann, G., Klecker, B., Bosqued, J. M., Reme, H., Balogh, A., Twitty, C., Mozer, F. S., Carlson, C. W., Mouikis, C., and Kistler, L. M.: Cluster observations of continuous reconnection at the magnetopause under steady interplanetary magnetic field conditions, Ann. Geophys., 22, 2355–2367, 2004,
SRef-ID: 1432-0576/ag/2004-22-2355.

Pinnock, M., Chisham, G., Coleman, I. J., Freeman, M. P., Hairston, M., and Villain, J.-P.: The location and rate of dayside reconnection during an interval of southward interplanetary magnetic field, Ann. Geophys., 21, 1467–1482, 2003,
SRef-ID: 1432-0576/ag/2003-21-1467.

Popescu, D., Sauvaud, J.-A., Fedorov, A., Budnik, E., Stenuit, H., and Moreau, T.: Evidence for a sunward flowing plasma layer adjacent to the tail high-latitude magnetopause during dawnward directed interplanetary magnetic field, J. Geophys. Res., 106, 29 479–29 490, 2001.

Reme, H., Aoustin, C., Bosqued, J., et al.: First multispacecraft ion measurements in and near the Earths magnetosphere with the identical Cluster ion spectrometry (CIS) experiment, Ann. Geophys., 19, 1303–1354, 2001,
SRef-ID: 1432-0576/ag/2001-19-1303.

Russell, C. T. and Elphic, R. C.: Initial ISEE magnetometer results – Magnetopause observations, Space Sci. Rev., 22, 681–715, 1978.

Safrankova, J., Nemecek, Z., Sibeck, D. G., Prech, L., Merka, J., and Santolik, O.: Two-point observation of high-latitude reconnection, Geophys. Res. Lett., 25, 4301–4304, 1998.

Sonnerup, B. U. Ö.: The Reconnecting Magnetosphere, in: ASSL Vol. 44, Magnetospheric Physics, 23–33, 1974.

Sonnerup, B. U. Ö., Paschmann, G., Papamastorakis, I., Sckopke, N., Haerendel, G., Bame, S. J., Asbridge, J. R., Gosling, J. T., and Russell, C. T.: Evidence for magnetic field reconnection at the earth's magnetopause, J. Geophys. Res., 86, 10 049–10 067, 1981.

Trattner, K. J., Fuselier, S. A., and Petrinec, S. M.: Location of the reconnection line for northward interplanetary magnetic field, J. Geophys. Res., 109, 3219–3229, 2004.

Paper II

A. Retinò, A. Vaivads, M. André, F. Sahraoui, Y. Khotyaintsev, J.S. Pickett, M. B. Bavassano Cattaneo, M. F. Marcucci, M. Morooka, C. J. Owen, S.C. Buchert, N. Cornilleau-Wehrlin

The structure of the separatrix region close to a magnetic reconnection X-line: Cluster observations.

Geophysical Research Letters , submitted, 2005.

The structure of the separatrix region close to a magnetic reconnection X-line: Cluster observations.

A. Retinò,[1] A. Vaivads,[1] M. André,[1] F. Sahraoui,[1,5] Y. Khotyaintsev,[1] J.S. Pickett,[3] M.B. Bavassano Cattaneo,[2] M.F. Marcucci,[2] M. Morooka,[1] C. J. Owen,[4] S.C. Buchert,[1] N. Cornilleau-Wehrlin[5]

We use Cluster spacecraft observations to study in detail the structure of a magnetic reconnection separatrix region on the magnetospheric side of the magnetopause. We concentrate on an event about 60 ion inertial lengths away from the X-line. The separatrix region has a width of several ion lengths and it contains subregions with widths of about an ion length. These subregions are highly structured down to Debye length scales. One subregion, a density cavity adjacent to the separatrix, has strong electric fields, accelerated electron beams and intense wave turbulence. Lower hybrid waves can be important for transport across a few subregions. We compare our observations with recent numerical simulations.

1. Introduction

Magnetic reconnection is a dominant process that allows the transfer of mass, momentum and energy from the solar wind into the magnetosphere [*Mozer et al.*, 2002]. Reconnection affects large volumes in space but is initiated at small scales. Therefore it is fundamental to study in detail its microphysics. Observations at ion and electron scales are few, especially near the X-line where spacecraft crossings are rare [*Øieroset et al.*, 2001; *Mozer et al.*, 2002]. In particular, coordinated high-time resolution particle and wave measurements close to the X-line have been reported only in a few cases [*Farrell et al.*, 2002; *Cattell et al.*, 2005]. The separatrices, the magnetic field lines connected to the X-line, have been identified near the X-line by *Øieroset et al.* [2001]; *Mozer et al.* [2002] but not described in detail. More detailed observations of the separatrices have been reported by *Cattell et al.* [2005] to provide evidence of electrostatic solitary waves and electron beams. Despite of these studies, detailed high-time resolution particle and field observations of the separatrices near the X-line are missing. Most of the information has instead been provided by numerical simulations of reconnection, e.g. *Hoshino et al.* [2001]; *Shay et al.* [2001]. Here we present and analyze high-time resolution particle and wave observations of a separatrix region (SR) on the magnetospheric side of the magnetopause (MP).

[1]Swedish Institute of Space Physics, Uppsala, Sweden.
[2]IFSI - INAF, Roma, Italy.
[3]University of Iowa, Iowa City, Iowa, USA.
[4]MSSL, University College London, United Kingdom.
[5]CETP - CNRS/IPSL, Vélizy France.

0094-8276/05/$5.00

2. Observations and analysis

We report Cluster small-scale observations close to an X-line at the high-latitude MP around 10:58:00 UT on 3 December 2001. The large-scale evidence of magnetic reconnection is shown in *Retinò et al.* [2005]. The vicinity to the X-line is substantiated by the observation of an ion jet reversal (Fig.3 in *Retinò et al.* [2005]). Reconnection occurs tailward of the cusp with northward IMF. The measured magnetic shear at the MP is about 160°. This should be close to the shear at the X-line because of the vicinity to the X-line. There is a large asymmetry between the magnetospheric density $\sim$1cm^{-3} and the magnetosheath (MSH) density $\sim$20cm^{-3}. Also there is a velocity shear $\sim$200km/s between the magnetosphere and the MSH flows. The ion and electron inertial lengths in the MSH are respectively $\lambda_{sh,i}$ $\sim$50km and $\lambda_{sh,e}$ $\sim$1km. Due to the large spacecraft separation, we use here observations only from SC/3.
We use data from several instruments onboard Cluster [*Escoubet et al.*, 2001]. We obtain an approximation of the plasma density N from the probe-to-spacecraft potential [*Pedersen et al.*, 2001].

2.1. Overall crossing close to the X-line

Fig.1 shows the overall passage of SC/3 close to the X-line. We concentrate on the interval 10:57:51.5–58:21 indicated by the yellow, magenta and blue layers. 10:57:51.5–58:02 SC/3 is in the SR (yellow layer). We describe this region in detail in the subsection 2.2. Then 10:58:02–58:16 SC/3 crosses the tailward jet region (magenta layer) where the ion velocity increases up to $\sim$500 km/s. Next 10:58:16–58:21 SC/3 crosses the rotational discontinuity (blue layer) where B_L changes sign from $B_L > 0$ (magnetospheric value) to $B_L < 0$ (MSH value) while $|B|$ stays roughly constant.
We compare our observations with a simulation of the reconnection layer in presence of a density asymmetry across the MP [*Nakamura and Scholer*, 2000]. To estimate the distance from the X-line we compare the widths of the jet region and of the rotational discontinuity in the data with those in the simulation (Fig.10 in *Nakamura and Scholer* [2000]) and we find an upper limit for the distance of $\sim 60\lambda_{sh,i} \approx$ 3000km. The main regions are recovered in the simulation but the observations show a more structured and dynamic reconnection layer. In particular magnetic structures with bipolar B_N are observed at 10:57:59 (in the SR on the magnetospheric side) and at 10:58:25, 10:58:35, 10:58:50 (on the MSH side) on a time scale of a few seconds. The polarity of B_N on both sides of the MP is consistent with these structures being bulges (micro FTEs) propagating away from the X-line.

2.2. Structure of the separatrix region

Fig.2 shows more detailed observations around the SR. During 10:57:45–57:51.5 SC/3 is in the magnetosphere. Around 10:57:51.5 SC/3 observes a sharp density gradient and a boundary in the DC and wave electric field E.

10:57:51.5–57:53 SC/3 is inside a density cavity where N depletes down to 0.2 times its magnetospheric level. In the density cavity the DC E increases up to ∼40mV/m, mainly in the positive normal direction i.e. from the magnetosphere to the MSH. The E fluctuations enhance and become broadband both around f_{lh} and f_{pe}. At 10:57:53 N starts to increase over the magnetospheric level while the DC E decreases. Next 10:57:53–57:56 $|B|$ changes from 50nT to 40nT. In this layer SC/3 observes broadband emission around f_{lh} with no clear peaks and localized emission at f_{pe}. Later 10:57:56–57:57 SC/3 crosses a steep density gradient, N increases up to ∼10cm^{-3}, where wave emission shows a strong peak at f_{lh} together with localized emission at f_{pe}. 10:57:57–58:01 SC/3 observes a magnetic structure with bipolar B_N and strong parallel currents at the edges. The wave activity observed at lower frequencies is decreased while at higher frequencies localized emission around f_{pe} is observed together with broadband emission. Finally 10:58:01–58:02 SC/3 is at the boundary with the reconnection jet where solitary structures start to be observed in WBD waveforms (not shown). In this time interval the WHISPER instrument was operating in active mode; the broadband emission up to 77kHz is most likely due to WHISPER interference. After 10:58:02 SC/3 is in the jet region.

On the magnetospheric side of the MP we define the SR as the layer between the magnetic separatrix and the reconnection jet. Topologically, the magnetic separatrix is the field line connected to the X-line. One possible way to identify the separatrix would be to take it as the boundary of first transmitted MSH electrons. For this event this cannot be done, the time resolution of the electron instrument is 4s while the whole SR is only ∼10s wide. The resolution of the wave instruments is higher, particulary that of the WBD (219.5kHz sampling rate). We therefore identify the magnetic separatrix at 10:57:51.5 when a sharp boundary is observed in WBD spectrogram where the wave emission becomes more intense and broadband. We in fact expect to see a change in the wave emission due to plasma instabilities caused by the arrival of the first transmitted electrons. With this definition the density cavity is just adjacent to the separatrix. We define the boundary with the jet region around 10:58:02 using the ion velocity. With this definition it roughly coincides with the region where solitary waves start to be observed (not shown). Note that because of the lower time resolution of the ion data (4s) this boundary is not sharp. We cannot say if the subregions observed in the SR are spatial or temporal structures because only data from SC/3 can be used at these small scales. We nevertheless interpret them as spatial structures, except for the bipolar magnetic structure at 10:57:57–58:01 that is interpreted as a bulge propagating away from the X-line. The SR has a width of ∼5$\lambda_{sh,i}$ while its subregions are ∼ $\lambda_{sh,i}$ wide. Our observations agree with a numerical simulation of magnetic reconnection by *Shay et al.* [2001]. As in the simulation we find a density cavity $\lambda_{sh,i}$ wide adjacent to the separatrix on the magnetospheric side of the MP with a strong DC E perpendicular to B. Nevertheless, the details of the SR are not resolved in the simulation.

Within the SR both broadband high frequency waves and localized Langmuir bursts often change properties inside WBD waveforms on a time scale of a few ms (not shown). This would correspond to a scale between $\lambda_{sh,e}$ and λ_{Debye} if they are interpreted as spatial structures. This evolution of the spectral properties of waves has not been reported in simulations.

Finally, electrostatic solitary waves are also observed on a time scale ∼0.1-0.2ms with amplitude ∼0.2-1mV/m (not shown). That time scale would correspond to a typical size ∼ λ_{Debye} assuming that their velocity is a fraction of the thermal electron energy ∼100eV [*Drake et al.*, 2003; *Cattell et al.*, 2005]. *Cattell et al.* [2005] report observations of such waves within a density cavity at the separatrix, together with waves at frequencies f_{lh}–f_{pe}. We observe solitary waves at the boundary between the SR and the reconnection jet

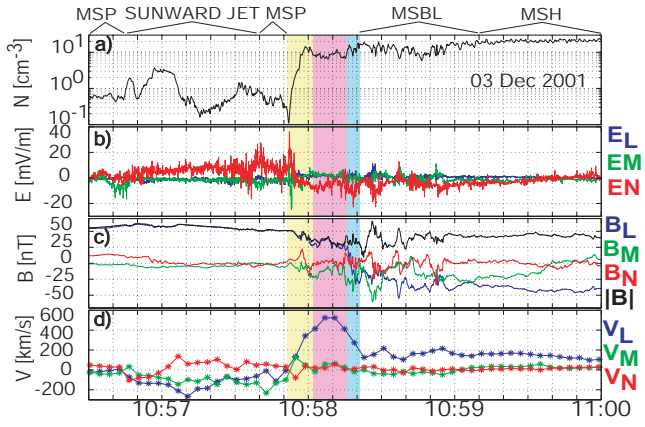

Figure 1. (a) plasma density, (b) electric field, (c) magnetic field, (d) ion velocity. The local MP frame (L, M, N) is obtained from minimum variance analysis of the magnetic field. The normal velocity of the MP V_N is obtained from the deHoffmann-Teller analysis (HT), $V_N = \overrightarrow{V}_{HT} \cdot \widehat{N}$ ≈20km/s with $\widehat{N}$=(0.79,0.42,-0.45)$_{GSE}$. In the frame moving with the MP 1s is then 20km∼0.5$\lambda_{sh,i}$. The magnetosphere (MSP), the sunward jet, the MSH boundary layer (MSBL) and the MSH are indicated. The yellow, magenta and blue vertical layers indicate the SR, the tailward jet region and the rotational discontinuity respectively.

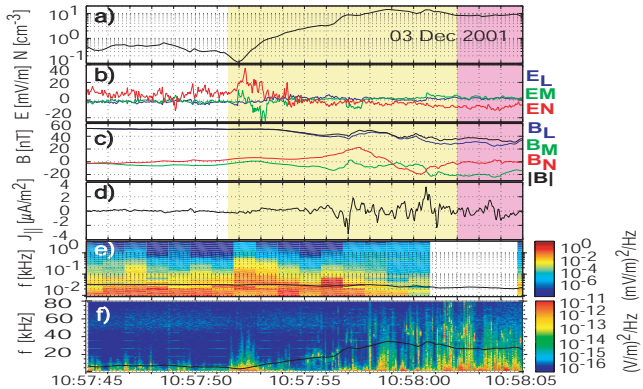

Figure 2. (a) density, (b) electric field, (c) magnetic field, (d) current density parallel to the magnetic field estimated using Ampere's law assuming a stationary and planar current sheet, (e) E spectrogram from STAFF/SA instrument, solid line shows the local lower hybrid frequency f_{lh}, (f) E spectrogram from WBD instrument, solid line shows the local plasma frequency f_{pe}. The SR is indicated in yellow. Data gap in STAFF/SA spectrogram corresponds to a time interval where WHISPER instrument was in active mode. Localized emissions around 45kHz between 10:58:01 and 10:58:03 in WBD spectrogram are due to WHISPER.

and throughout most of the jet region, but not within the SR.
In summary, we have identified the SR and shown that it is highly structured down to the smallest scales. The observations are generally in agreement with numerical simulations except for some features at small scales.

2.3. Wave-particle interaction

For this event we obtain for the first time simultaneous high-time resolution measurements of E spectra and electron distribution functions $f_e(\mathcal{E})$ in the SR, see Fig.3; $\mathcal{E}$ is the energy. Around 10:57:52 (in the density cavity) the E spectrum at lower frequencies shows two peaks around f_{lh} and broadband emission up to about 4kHz. At higher frequencies the E spectrum shows a peak around f_{pe} ∼4kHz and then again broadband emission up to ∼20kHz. The broad peak around 60kHz (also observed at the next two times) is due to a type III solar burst and is not a local emission. The $f_e(\mathcal{E})$ is the largest at 0° for $\mathcal{E} > 300$eV and at 180° for $\mathcal{E} < 100$eV. There is a beam in the parallel direction of few hundreds eV having a positive slope in the $f_e(\mathcal{E})$. This energy corresponds roughly to the local electron Alfvén velocity $V_{A,e}$. At the next time interval, around 10:57:54, there is no clear peak at f_{lh} and there is a broad peak around f_{pe} ∼10kHz. The $f_e(\mathcal{E})$ is the largest at 0° for $\mathcal{E} < 100$eV while is isotropic for $\mathcal{E} > 200$eV. Finally around 10:57:56, the E spectrum shows a very strong peak at f_{lh} and again a broad peak at f_{pe} ∼20kHz. The $f_e(\mathcal{E})$ is similar to that at 10:57:54, the phase space density is larger because N has increased. Note the differences between the E spectra and the $f_e(\mathcal{E})$ in the three subregions. At lower frequencies, i.e. below f_{pe}, the emission is broadband everywhere but with higher amplitude in the density cavity. At higher frequencies the emission in the cavity is much more broadband than in the others subregions. The slope of the spectrum below and above f_{pe} in the cavity is clearly different. An electron beam is observed only in the cavity.
Fig.4 is a sketch of the reconnection geometry, the main regions crossed by SC/3 are indicated with the same colors used in Fig.1. A zoom of the SR (yellow region) is shown in the inset together with its fine structures.
To investigate the wave-particle interaction in the SR we compare our observations with a magnetic reconnection simulation by *Hoshino et al.* [2001]. Note that the simulation is limited to a distance $\sim 10\lambda_{sh,i}$ from the X-line while our observations are probably obtained further away; also the simulation describes symmetric reconnection. We compare the E spectrum and the $f_e(\mathcal{E})$ in the density cavity with those close to the magnetic separatrix in the simulation and find a good agreement. The E spectrum (bottom left panel, Fig.7 in *Hoshino et al.* [2001], dashed line) shows a sharp peak at the local f_{pe} together with a significant power in the lower frequency range (below f_{pe}), consistent with observations. Also the different spectrum slopes below and above f_{pe} are consistent with observations. The $f_e(\mathcal{E})$ in the simulation (top left panel, Fig.5 in *Hoshino et al.* [2001]) shows bi-streaming cold and hot electron populations flowing toward and away from the X-line respectively, consistent with observations. *Hoshino et al.* [2001] find that the beam flowing away from the X-line reaches velocity up to the electron Alfvén velocity $V_{A,e}$, as in the observations. They interpret the cold electrons as convected toward the X-line without crossing it while the hot electrons as accelerated away from the X-line. In our observations of asymmetric reconnection the observed electron beam could correspond to MSH electrons accelerated away from the X-line on the magnetospheric side of the MP. We also compare the E spectrum and the $f_e(\mathcal{E})$ in the other two subregions with those downstream of the magnetic separatrix in the simulation. The comparison is less straightforward than above, the subregions in the simulation do not correspond exactly to the subregions observed around 10:57:54 and 10:57:56. The E spectrum (top left panel, Fig.7 in *Hoshino et al.* [2001], dashed line) shows in the lower frequency range less power than that found close to the separatrix and broader peaks around the local f_{pe}, in agreement with our observations. No strong emission exists at lower frequencies in the simulation while we find a peak at f_{lh} around 10:57:56 . The $f_e(\mathcal{E})$ is isotropic at high energies as in the observations. In summary, our observations of wave-particle interactions inside the SR agree with the simulation by *Hoshino et al.* [2001] although the match between the subregions in the simulation and the observed ones is not perfect.

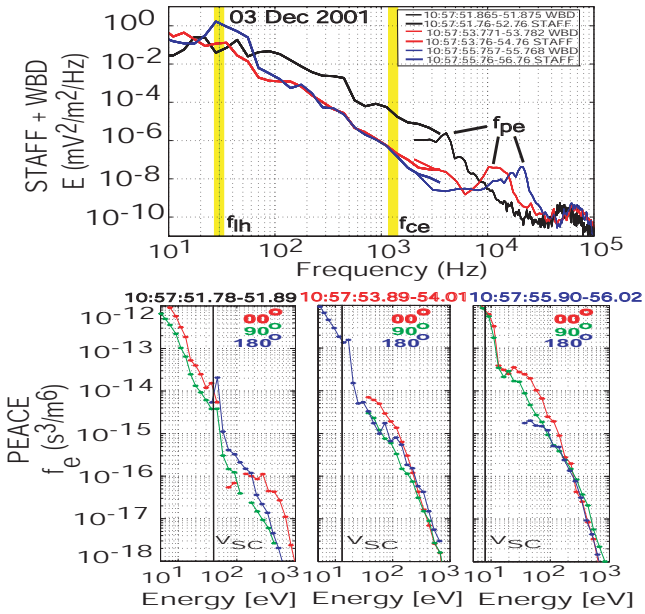

Figure 3. Upper panel: electric field spectra measured by SC/3 around 10:57:52, 10:57:54 and 10:57:56. Time intervals over which spectra are calculated are shown in the legend. The spectral ranges of f_{lh} and of the electron cyclotron frequency f_{ce} are marked yellow while f_{pe} is shown with black lines. Lower panel: $f_e(\mathcal{E})$ for three different pitch angles measured within 118ms every 2s around the same times as E spectra. 0° is away and 180° towards the X-line. The black vertical line is the energy corresponding to the spacecraft potential. Gaps in solid lines correspond to zero counts.

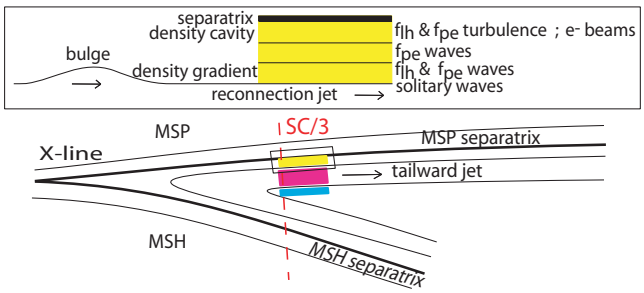

Figure 4. A sketch of the reconnection geometry. A zoom of the SR is shown in the inset.

As suggested by *Hoshino et al.* [2001] lower hybrid (LH) waves can be important in scattering electrons. In a case study *Vaivads et al.* [2004] show that transport due to waves with frequencies around f_{lh} is efficient across thin layers interpreted as separatrices. Here we estimate the anomalous collision frequency between electrons and LH waves as $\nu^* \sim (\omega_{pe}^2/\omega_{lh})\epsilon_0\delta E^2/2nk_BT_e$ according to *Coroniti* [1985]. In the density cavity we take f_{pe} ∼4kHz, f_{lh} ∼30Hz, n ∼0.1cm^{-3}, k_BT_e ∼100eV, δE^2 ∼2mV$^2/m^2$ and we obtain ν^* ∼2Hz. A similar estimation at the density gradient (around 10:57:56) where a strong peak at f_{lh} is observed gives ν^* ∼20Hz. The estimated ν^* in the two subregions is close to the local f_{lh} (20–30Hz within the SR) suggesting that LH waves are important for transport there. The transport could be important across the entire SR but a more detailed analysis is necessary to confirm this point.

3. Conclusions

We present detailed observations of a magnetic reconnection separatrix region on the magnetospheric side of the magnetopause. We summarize our results as follows:

1. A separatrix region several $\lambda_{sh,i}$ wide can be identified between the magnetic separatrix and the reconnection jet. This region contains a few subregions each about $\lambda_{sh,i}$ wide. These subregions are highly structured with scales down to λ_{Debye} in the electric field even though the X-line can be up to ∼60$\lambda_{sh,i}$ away. Electrostatic solitary waves are observed at the boundary between the separatrix region and the reconnection jet, inside most part of the reconnection jet, but not within the separatrix region.

2. We find that the density cavity observed adjacent to the magnetic separatrix is a region of strong DC electric fields, broadband turbulence around both f_{lh} and f_{pe} and electron beams accelerated away from the X-line.

3. Lower hybrid waves can be important for transport across a few subregions within the separatrix region.

4. Our observations generally agree with recent numerical simulations although some of the observed features are not resolved in the simulations.

Acknowledgments. A. Retinò is supported by the Swedish National Space Board. J.S. Pickett acknowledges the support of NASA GSFC through Grant NNG04GB98G. Discussion with P. Canu is acknowledged.

References

Cattell, C., et al., Cluster observations of electron holes in association with magnetotail reconnection and comparison to simulations, *J. Geophys. Res.*, *110*, 1211–1226, 2005.

Coroniti, F. V., Space plasma turbulent dissipation - Reality or myth?, *Space Sci. Rev.*, *42*, 399–410, 1985.

Drake, J. F., M. Swisdak, C. Cattell, M. A. Shay, B. N. Rogers, and A. Zeiler, Formation of Electron Holes and Particle Energization During Magnetic Reconnection, *Science*, *299*, 873–877, 2003.

Escoubet, C., M. Fehringer, and M. Goldstein, The Cluster mission, *Ann. Geophys.*, *19*, 1197–1200, 2001.

Farrell, W. M., M. D. Desch, M. L. Kaiser, and K. Goetz, The dominance of electron plasma waves near a reconnection X-line region, *Geophys. Res. Lett.*, *29*, 8–11, 2002.

Hoshino, M., K. Hiraide, and T. Mukai, Strong electron heating and non-Maxwellian behavior in magnetic reconnection, *Earth Planets Space*, *53*, 627–634, 2001.

Mozer, F. S., S. D. Bale, and T. D. Phan, Evidence of Diffusion Regions at a Subsolar Magnetopause Crossing, *Phys. Rev. Lett.*, *89*(1), 015,002–+, 2002.

Nakamura, M., and M. Scholer, Structure of the magnetopause reconnection layer and of flux transfer events: Ion kinetic effects, *J. Geophys. Res.*, *105*, 23,179–23,192, 2000.

Øieroset, M., T. D. Phan, M. Fujimoto, R. P. Lin, and R. P. Lepping, In situ detection of collisionless reconnection in the Earth's magnetotail, *Nature*, *412*, 414–417, 2001.

Pedersen, A., et al., Four-point high time resolution information on electron densities by the electric field experiments (EFW) on Cluster, *Ann. Geophys.*, *19*, 1483–1489, 2001.

Retinò, A., et al., Cluster multispacecraft observations at the high-latitude duskside magnetopause: implications for continuous and component magnetic reconnection, *Ann. Geophys.*, *23*, 461–473, 2005.

Shay, M. A., J. F. Drake, B. N. Rogers, and R. E. Denton, Alfvénic collisionless magnetic reconnection and the Hall term, *J. Geophys. Res.*, *106*, 3759–3772, 2001.

Vaivads, A., M. André, S. C. Buchert, J.-E. Wahlund, A. N. Fazakerley, and N. Cornilleau-Wehrlin, Cluster observations of lower hybrid turbulence within thin layers at the magnetopause, *Geophys. Res. Lett.,* , *31*, 3804–3807, 2004.

A. Retinò, Swedish Institute of Space Physics, Box 537, SE-75121 Uppsala, Sweden. (alessandro.retino@irfu.se)